

See discussions, stats, and author profiles for this publication at: <https://www.researchgate.net/publication/258060254>

Novel polyamine analogues: From substrates towards potential inhibitors of monoamine oxidases

ARTICLE *in* EUROPEAN JOURNAL OF MEDICINAL CHEMISTRY · OCTOBER 2013

Impact Factor: 3.45 · DOI: 10.1016/j.ejmech.2013.07.005 · Source: PubMed

CITATIONS

4

READS

51

10 AUTHORS, INCLUDING:



Giorgio Cozza

University of Padova

64 PUBLICATIONS 1,116 CITATIONS

SEE PROFILE



Patrizia Hrelia

University of Bologna

206 PUBLICATIONS 3,446 CITATIONS

SEE PROFILE



Anna Minarini

University of Bologna

97 PUBLICATIONS 2,007 CITATIONS

SEE PROFILE



Maria Luisa Di Paolo

University of Padova

41 PUBLICATIONS 488 CITATIONS

SEE PROFILE



Original article

Novel polyamine analogues: From substrates towards potential inhibitors of monoamine oxidases



Emanuela Bonaiuto^a, Andrea Milelli^b, Giorgio Cozza^c, Vincenzo Tumiatti^b, Chiara Marchetti^d, Enzo Agostinelli^{e,f}, Carmela Fimognari^b, Patrizia Hrelia^d, Anna Minarini^{d,**}, Maria Luisa Di Paolo^{a,g,*}

^a Department of Molecular Medicine, University of Padova, Via G. Colombo 3, 35131 Padova, Italy

^b Department for Life Quality Studies, University of Bologna, Rimini Campus, 47921 Rimini, Italy

^c Department of Biomedical Sciences, University of Padova, 35131 Padova, Italy

^d Department of Pharmacy and Biotechnology, University of Bologna, Via Belmeloro 6, 40126 Bologna, Italy

^e Istituto Pasteur-Fondazione Cenci Bolognietti, Department of Biochemical Sciences "A. Rossi Fanelli", SAPIENZA University of Rome, 00185 Rome, Italy

^f CNR, Institute Biology and Molecular Pathology, P.le Aldo Moro 5, 00185 Rome, Italy

^g Consorzio Interuniversitario "Istituto Nazionale Biostrutture e Biosistemi", 00136 Roma, Italy

ARTICLE INFO

Article history:

Received 2 May 2013

Received in revised form

9 July 2013

Accepted 12 July 2013

Available online 1 October 2013

Keywords:

Monoamine oxidase (MAO)

Inhibitors

Isothiocyanate

Polyamine derivatives

Docking studies

ABSTRACT

New polyamine derivatives **1–8**, related to the previously reported *N*¹,*N*¹²-dibenzyl-dodecane-1,12-diamine (Bis-Bza-Diado) and *N*¹-benzyl-spermine (BD6), have been synthesized and used as "probes" (potential substrates or inhibitors) of the human monoamine oxidases (MAO A and MAO B) and Vascular-Adhesion-protein – 1 (VAP-1). Compound **8**, the most effective inhibitor of the series, is characterized by a 12-methylene carbon chain ending with an isothiocyanate (ITC) group. Interestingly, it behaves as competitive inhibitor of MAO B and as irreversible inhibitor of MAO A. Compound **3**, an asymmetric spermine analogue bearing a thiophene ring, acts as a reversible mixed inhibitor, selective for MAO B (*K*_{IE} = 23 μM). Docking studies performed using the available Protein Data Bank (PDB) structures of MAO A and MAO B, suggested that the different mode of inhibition of **8** may be explained by the different binding poses of **8** into the active site cavities of the two MAO isoforms. The ε-amino group of Lys 305 of MAO A is proposed as possible target of the ITC group of the inhibitor. Further studies are in progress to confirm this hypothesis.

These results indicate a potential use of the polyamine scaffold for the development of new MAO inhibitors for application in human pathologies involving these enzymes.

© 2013 Elsevier Masson SAS. All rights reserved.

1. Introduction

Monoamine oxidase A and B (MAO A and MAO B) are FAD-containing enzymes bound to the mitochondrial outer membrane, which play essential roles in the catabolism of amine

neurotransmitters in the brain and peripheral tissues. MAO A is more specific for serotonin, MAO B for benzylamine (BZA) and β-phenylethylamine, while both MAO isoforms are active against dopamine, adrenaline and noradrenaline. An increase of oxidative deamination catalysed by MAOs may lead both to a depletion of the neurotransmitter levels and to an overproduction of their by-products (hydrogen peroxide and aldehydes), which contribute to the development of an inflammatory and "oxidative stress" condition, generally associated to the initial stage and to the progression of neurodegeneration [1–4].

For these reasons, MAO A and MAO B are well-known targets of anti-neurodegenerative and anti-depressant therapies: MAO B mainly in Parkinson's and Alzheimer's diseases, while MAO A mainly in affective disorders [2,4].

Many MAO inhibitors have been developed and some of them are "old" drugs in clinical use, such as the anti-depressant,

Abbreviations: BZA, benzylamine; tyramine, *p*-tyramine; MAO, monoamine oxidase; VAP-1, semicarbazide-sensitive amine oxidase/vascular-adhesion-protein-1; Bis-Bza-Diado, *N*¹,*N*¹²-dibenzyl-dodecane-1,12-diamine; BD6, *N*¹-(3-aminopropyl)-*N*⁴-(3-(benzylamino)propyl)butane-1,4-diamine/*N*¹-benzyl-spermine; ITC, isothiocyanate; AITC, allyl isothiocyanate; *K*_{IE}, enzyme–inhibitor dissociation constant/inhibition constant; *K*_{IES}, enzyme–substrate complex–inhibitor dissociation constant; *K*_m, Michaelis–Menten constant; *V*_{max}, maximum velocity.

* Corresponding author. Dept. of Molecular Medicine, University of Padova, Via G. Colombo 3, 35131 Padova, Italy. Tel.: +39 (0)49 8276119; fax: +39 (0)49 8073310.

** Corresponding author. Tel.: +39 (0)51 2099709.

E-mail addresses: anna.minarini@unibo.it (A. Minarini), marialuisa.dipaolo@unipd.it (M.L. Di Paolo).

irreversible MAO A inhibitor clorgyline and the antiparkinson, MAO-B irreversible inhibitors selegiline and rasagiline [2,5]. Most of the irreversible inhibitors are characterized by a propargylamine moiety, able to inactivate the FAD cofactor, and may cause side effects. To overcome this problem, new generations of inhibitors, such as the reversible MAO A inhibitors moclobemide and taloxatone were developed [5,6]. Additionally, recent findings on neuroprotective properties of some MAO inhibitors [2,6–8], have been a spur to develop novel MAO inhibitors. Although the drug discovery in this field has been focused mainly to treat neurological disorders, MAO A inhibitors might find a new application in treating different pathological conditions, such as prostate cancer; actually, it was identified high expression of MAO A in normal basal prostatic epithelium and high-grade primary prostate cancer [9,10].

In the last years, the renewed interest for MAO inhibitors has produced many patents: novel structures, such as pyrazole derivatives, hydrazine-based compounds and other heterocycles, such as chromones and chalcones, have been used as scaffolds and proposed for potential pharmacological applications, in particular in neurodegenerative diseases [5,9,11–14].

Little information is available about the effect of polyamine derivatives as MAO inhibitors. In our recent paper, we reported the MAO inhibitory activities of *N*¹,*N*¹²-dibenzyldecane-1,12-diamine (Bis-Bza-Diado) and of *N*¹-benzyl-spermine (BD6) [15]. In particular, we found that Bis-Bza-Diado behaved as a reversible, although weak MAO B inhibitor ($K_i = 130 \mu\text{M}$ [15];). The polycationic structure of polyamines allows them to interact with a variety of cellular targets, which may be either activated or inhibited, suggesting that polyamine research is an important field for drug development with great potential for identifying new molecules for different diseases. Polyamine-based analogues have shown potential as

antiproliferative [16], antiparasitic, antibacterial, and anti neurodegenerative [17] agents and could also be used as probes to investigate the role of cellular processes regulated by enzymes or transcription [18].

Based on our previous results, the aim of this study was to investigate the structural features required to improve the interactions of a polyamine scaffold with the MAO active sites. It was verified that it is possible to modulate both affinity and selectivity for diverse biological targets by inserting different groups onto a polymethylene backbone, as well as appropriate spacers separating the amine functions [19,20]. Thus, using BD6 and Bis-Bza-Diado as lead compounds, eight novel polyamine derivatives (1–8) were designed and synthesized to be tested as substrates or inhibitors of different types of amine oxidases, as potential therapeutic targets.

Firstly, the compounds were evaluated as potential substrates of both human MAOs and semicarbazide-sensitive amine oxidase named vascular-adhesion-protein-1 (VAP-1). VAP-1 is a human AO involved in the inflammatory processes and various disorders [21], and whose circulating form was found increased in plasma of patients with Alzheimer's disease [22,23]. The compounds which did not act as substrates were then tested as potential inhibitors.

The drug design and molecular structures of polyamines 1–8 are shown in Fig. 1.

The structure modifications applied to BD6 and Bis-Bza-Diado concerned both aromatic rings and nitrogen atoms, in order to improve the negligible activity of MAOs on spermine and the weak inhibitory effect of the two polyamine derivatives BD6 and Bis-Bza-Diado on MAO B [15].

To this aim we replaced the benzyl group of BD6 by different aromatic ring, such as naphthalene, pyridine and thiophene, providing compounds 1, 2, and 3, respectively. By a kinetic

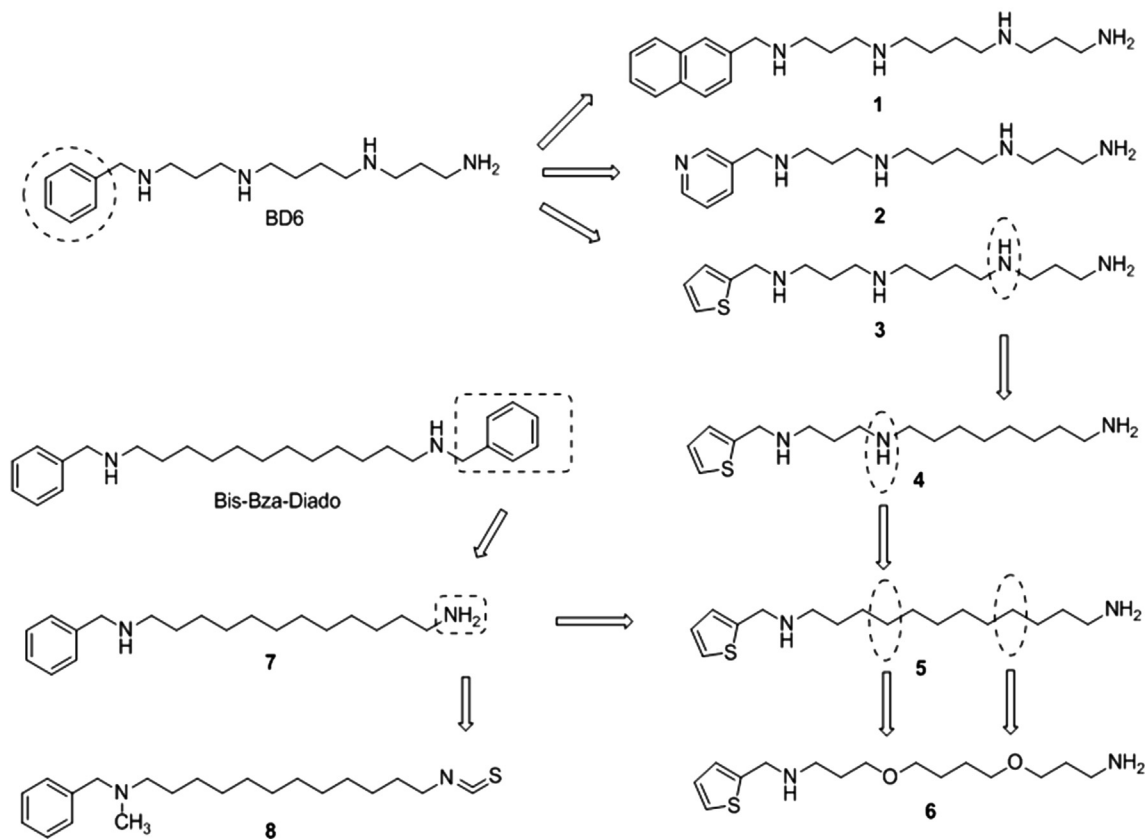
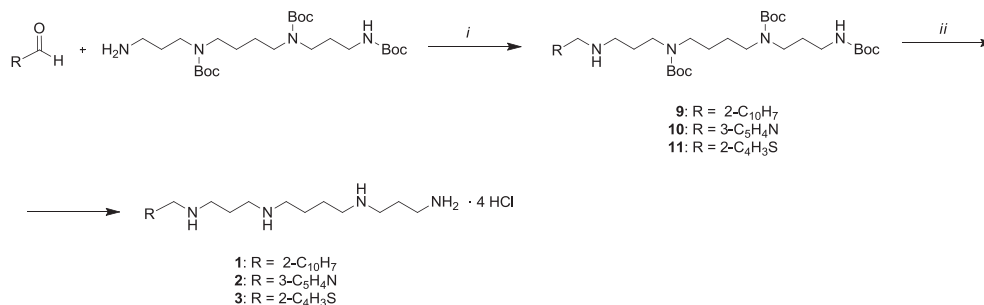


Fig. 1. Drug design of compounds 1–8, starting from BD6 and Bis-Bza-Diado.



Scheme 1. (i) (a) Toluene, reflux, 3 h, (b) NaBH₄, EtOH, rt, 4 h, 81–90% yields; (ii) HCl 3 M, rt, overnight, quantitative yields, Boc = (CH₃)₃COCO–.

approach, we found that **3** behaved as a novel reversible and mixed-competitive inhibitor of MAO B. To evaluate the importance of a polycationic chain in favour of amine oxidase activity, the inner nitrogen atoms of the spermine portion of **3** were replaced with one or two methylene groups, affording **4** and **5**, respectively, or with oxygen atoms to give compound **6**.

Additionally, as we found the symmetric substituted diamine Bis-Bza-Diado behaving as a reversible MAO B inhibitor, we investigated the importance of the benzyl moiety for this activity, by synthesizing the mono benzyl-diamine **7**.

Furthermore, to gain insight on the ligand binding site(s) and structural features for MAO inhibition, we designed and synthesized compound **8** in which the primary amine group of the *N*-methyl derivative of **7**, that is the intermediate **24** (Scheme 4), was substituted with an isothiocyanate (ITC) moiety as an electrophilic reactive group capable of interacting irreversibly with a suitably located nucleophilic amino acid residue at or near the binding site. The insertion of the methyl group in **7** to give **24**, was necessary to prevent an intramolecular reaction between its secondary amino group and –NCS. However, we found that this modification did not significantly alter the biological profile of **7**.

Since compound **8** inhibited both MAOs with similar dissociation constant values but with different mechanisms, that is competitive inhibition of MAO B and irreversible inhibition of MAO A, computational and docking studies were performed to rationalize and to understand the different binding mode of **8** to human MAOs.

Finally, in order to identify whether the effect of **8** on MAOs was due to the presence of the ITC group, we assessed the MAO inhibitory activity of two ITC natural compounds, allyl isothiocyanate (AITC) and sulforaphane, for comparison. To note that, due to the presence of the ITC group in their structures, AITC and sulforaphane, occurring primarily in cruciferous vegetables, are endowed with significant anti-proliferative and cancer chemopreventive activities [24–27]. For this reason, we thought of interest to include in the present paper the study of the cytotoxic effects of compounds **7** and **8** on human neuroblastoma SH-SY5Y cells, to have a comparison with cytotoxicity of sulforaphane [28].

2. Results and discussion

2.1. Chemistry

Diamine Bis-Bza-Diado and tetraamine BD6 were synthesized as previously reported [15]. Tetraamines **1**, **2** and **3** were synthesized as reported in Scheme 1: the appropriate aldehydes were reacted with tri-Boc-spermine [29] to afford the corresponding Schiff bases which were reduced *in situ* to give compounds **9–11**; acidic deprotection of such compounds led to the corresponding tetraamines **1–3** as tetrahydrochloride salts.

Triamine **4** was synthesized as reported in Scheme 2: *N*-protected aminoalcohol **12** [30] was activated with tosyl chloride to give **13** which, reacting with the mono-Boc protected 1,8-diaminooctane **14** [31] furnished the intermediate **15**. Basic deprotection of the trifluoroacetyl group led to the diamine **16** that was reacted with 2-thiophenecarboxaldehyde to afford the corresponding Schiff base which was reduced *in situ* to give compound **17**; acidic deprotection of such compound led to the corresponding triamine **4** as trihydrochloride salt.

For the synthesis of the diamines **5** and **6** (Scheme 3), 2-thiophenecarboxaldehyde was reacted with the appropriate mono-Boc-diamine **18** [31] or **19** [32] to afford the corresponding Schiff bases which were reduced *in situ* to give compounds **20** and **21**, respectively; acidic deprotection of such compounds led to the corresponding diamines **5** and **6** as dihydrochloride salts, respectively.

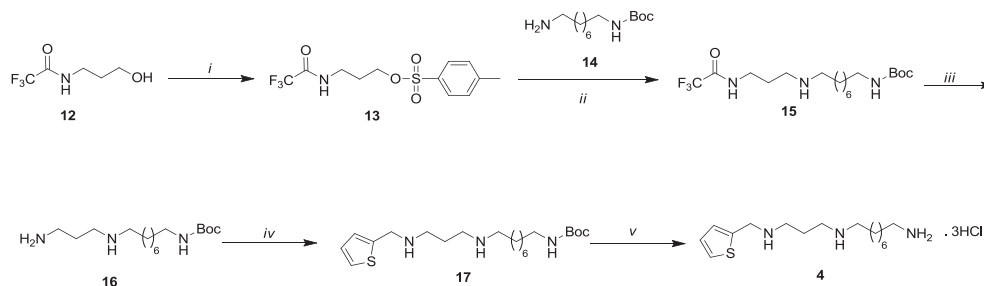
Compound **7** was synthesized as previously reported [15] for Bis-Bza-Diado, using a 1:1 stoichiometry of 1,12-diaminododecane and benzaldehyde. For the synthesis of **8**, to avoid an intramolecular reaction between –NCS and secondary amino group, it was necessary to transform the last one in tertiary amine. **8** was synthesized starting from the protection of the primary amine of **7** as trifluoroacetyl **22** (Scheme 4); Eschweiler–Clark methylation of the secondary amine of **22** led to compound **23**; removal of the trifluoroacetyl protecting group through basic hydrolysis led to **24** which was reacted with 1,1'-thiocarbonyldi-2(1*H*)-pyridone to provide the corresponding isothiocyanate **8** [33] (NMR Spectra in Fig. S1, Supplementary information).

2.2. Biochemistry

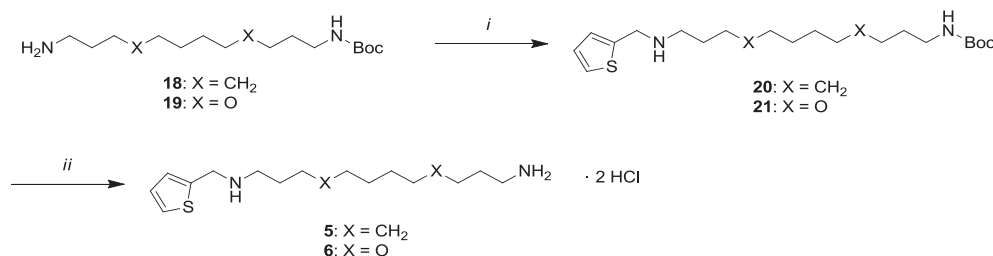
2.2.1. Potential substrates of human MAOs and VAP-1

Compounds **1–8** were firstly assayed as potential substrates for human VAP-1, MAO A and MAO B. Only compounds **4–7** behaved as substrates and their kinetic parameters are reported in Table 1. All the AOs showed a very good affinity for **7** (*K_m* values from 5 to 50 μM), but only VAP-1 and MAO B showed high catalytic efficiency (*K_m/V_{max}*) and *V_{max}* values, in comparison with their “standard” substrate (BZA). In particular, the catalytic efficiency of VAP-1 for **7** was similar to that for 1,12-diaminododecane [34]. To verify whether the methylation of the secondary amine group of **7** could affect its biological profile, we also tested the intermediate **24** (Table 1). This modification reduced slightly the affinity and catalytic efficiency for VAP-1, improved the affinity for MAO B in comparison to **7** (*K_{m24}* < *K_{m7}*) but decreased its relative *V_{max}*, while it did not significantly change the kinetic parameters for MAO A.

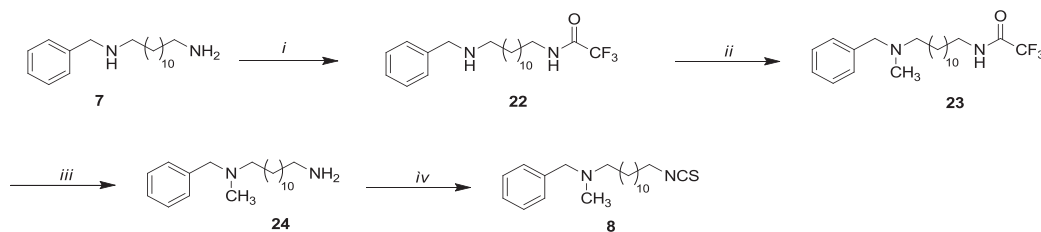
The substitution of the benzyl moiety of the diamine **7** with a thiophene ring, affording **5**, did not improve nor affinity neither catalytic efficiency of MAO A and VAP-1 respect to **7**. Differently, MAO B showed a better affinity (lower *K_m* value) and lower *V_{max}* for **5** than **7**, indicating that the thiophene ring ameliorated the



Scheme 2. (i) Tosyl chloride, Et₃N, DCM, rt, overnight, 58% yield; (ii) THF, reflux, 4 h, 41% yield; (iii) NaOH 40%, MeOH, rt, overnight, quantitative yield; (iv) (a) 2-CHO-C₄H₉S, toluene, reflux, 3 h, (b) NaBH₄, EtOH, rt, 4 h, 77% yield; (v) HCl 3 M, rt, overnight, quantitative, yield. Boc = (CH₃)₃COCO-.



Scheme 3. (i) (a) 2-CHO-C₄H₉S, toluene, reflux, 3 h, (b) NaBH₄, EtOH, rt, 4h, 59–70% yields; (ii) HCl 3 M, rt, overnight, quantitative yields, Boc = (CH₃)₃COCO-.



Scheme 4. (i) CF₃CO₂Et, MeOH, -78 °C, 1 h, 86% yield; (ii) HCOOH 85%/HCHO 40%, reflux, 24 h, 93% yield; (iii) K₂CO₃, MeOH/H₂O, reflux, 2 h, 70% yield; (iv) 1,1'-thiocarbonyldi-2(1H)-pyridone, DCM, N₂, rt, overnight, 59% yield.

interaction with MAO B active site cavity, but not the following chemical step of catalysis.

No amine oxidase activity was found on spermine derivatives **1–3**, in agreement with the known negligible spermine activities of MAOs and VAP-1. The replacement of one amine group of the spermine portion of **3** with a methylene group, affording **4**, determined a partial recovery, respect to **3**, only of VAP-1 activity. The introduction of two oxygen atoms in place of the two inner nitrogen atoms of spermine affording **6**, determined a further improvement of amine oxidase activity of VAP-1 and of MAO B, but with an affinity and catalytic efficiency lower than those of **5**. These results indicate that the inner 12 methylene chain in this compound is a very important structural feature to improve its affinity, not only for VAP-1 [34], but also for human MAOs. This behaviour is probably due to a strong interaction of the aliphatic chain of the compound with the hydrophobic binding site cavities of the MAOs [35] and is in good agreement with previous studies regarding the increased affinity for MAO B observed by lengthening the aliphatic chain of BZA to phenethylamine [36]. Additionally, in the case of MAO A, these strong apolar interactions might affect the catalytic steps (low V_{\max} values for **5**, **7** and **24**), for example, slowing down the exit of the reaction product (aldehyde).

Recent studies reported about the insulin-like effect of the VAP-1 and MAO activity in adipocytes and proposed the use of amine oxidases substrates for anti-diabetic therapies, particularly in

insulin-resistant conditions [37–39]. Thus, our novel substrates might be of interest for their potential development in this field.

2.2.2. Screening and selection of potential inhibitors

Compounds included in Fig. 1 which did not behave as AO substrates were tested as potential inhibitors of MAOs and VAP-1. Bis-Bza-Diado, BD6 and spermine were also tested as reference compounds. The kinetic parameters were determined in the presence of 200 μ M of the selected compounds, after a pre-incubation time of about 30 min. A control sample was run under the same experimental conditions. The residual V_{\max} and catalytic efficiency (V_{\max}/K_m), relatively to control sample, were reported in Table 2.

Among Bis-Bza-Diado derivatives, compound **8**, bearing a terminal ITC group, emerged as the most effective in inhibiting both MAO A and MAO B activities (no detectable residual activity). Interestingly, the substitution of the primary amine group of **24** with an ITC moiety, switched a very good substrate (**24**) in a “good” inhibitor (**8**).

Among the derivatives of BD6, characterized by a spermine moiety, **3** appeared to be the most effective and selective compound in inhibiting MAO B activity (residual V_{\max}/K_m about 5% and 57% for MAO B and A, respectively). This behaviour is in agreement with the high affinity of MAO B for **5**, the substrate containing the same thiophene ring on the terminal amine function.

Table 1
Polyamine derivatives **4–7** and **24** acting as substrates of human VAP-1 and MAOs.

Substrate	VAP-1			MAO A			MAO B		
	K_m (μ M)	Relative V_{max}/K_m^a	Relative V_{max}^a	K_m (μ M)	Relative V_{max}/K_m^a	Relative V_{max}^a	K_m (μ M)	Relative V_{max}/K_m^a	Relative V_{max}^a
4	1730 \pm 230	0.09	0.38	n.a. ^b	n.a. ^b	n.a. ^b	n.a. ^b	n.a. ^b	n.a. ^b
5	11 \pm 4	35	1.77	80 \pm 9	0.29	0.10	18 \pm 6	12	0.53
6	350 \pm 50	0.87	0.71	>>1200	0.06	n.d. ^c	401 \pm 94	0.21	0.19
7	5 \pm 1	80	1.88	43 \pm 17	0.40	0.08	50 \pm 22	18.6	1
24	9 \pm 2	30	0.73	44 \pm 11	0.60	0.03	12 \pm 4	17.5	0.24

^a Standard substrate: BZA for VAP-1 ($V_{max} = 221 \pm 12$ nmol H_2O_2 min⁻¹ mg⁻¹; $K_m = 224 \pm 40$ μ M; $V_{max}/K_m = 0.99$ ml min⁻¹ mg⁻¹) and MAO B ($V_{max} = 5.9 \pm 0.1$ nmol H_2O_2 min⁻¹ mg⁻¹, $K_m = 455 \pm 50$ μ M; $V_{max}/K_m = 0.013$ ml min⁻¹ mg⁻¹); tyramine for MAO A ($V_{max} = 71 \pm 3$ nmol H_2O_2 min⁻¹ mg⁻¹, $K_m = 451 \pm 36$ μ M; $V_{max}/K_m = 0.157$ ml min⁻¹ mg⁻¹).

^b No significant activity: relative activity lower than 0.01 at 500 μ M of the tested compound.

^c Not determinable.

None of the tested compounds were found to be more effective than Bis-Bza-Diado in inhibiting VAP-1 activity. Additionally, Bis-Bza-Diado was found to be also the second most effective in inhibiting the activity of MAO A (residual catalytic efficiency about 29%), in agreement with the high affinity of its monosubstituted analogue **7**, acting as MAO A substrate ($K_m = 40$ μ M, Table 1).

On the basis of this screening, we focused our further kinetic studies on MAOs and on compounds more effective in inhibiting their activities (**3**, **8** and Bis-Bza-Diado).

2.2.3. Mode of inhibition of Bis-Bza-Diado and **3** versus MAO A and MAO B

To study the type of inhibition of Bis-Bza-Diado and **3** on MAOs, kinetic parameters (V_{max} , K_m and V_{max}/K_m) of MAO A and MAO B were determined in the presence of various concentrations of these compounds, using tyramine and BZA, respectively, as substrates. BD6, precursor of compound **3** and isatin, a non-selective reversible MAO inhibitor, were used as reference compounds. Enzymes were pre-incubated with the tested compound for about 30 min, before adding substrate. In Fig. 2, the plots of initial rate of reaction vs substrate concentration in the presence of **3** are shown, as examples. The mode of inhibition and the inhibition constant values were determined by the global fit analysis of the kinetic data, performed with the GraphPad Prism software 5.0 or Sigma Plot 9.0. The inhibition data and selectivity are reported in Table 3. Bis-Bza-Diado, and **3** behaved according to a mixed mode of inhibition, (they affected both K_m and V_{max} values), and both the compounds

had a better affinity for the free enzyme than for the enzyme–substrate complex, being their $K_{IE} < K_{IES}$.

Bis-Bza-Diado appeared little more selective for MAO A (about 2 fold), while compound **3** preferred MAO B, with a higher selectivity (about 10 fold) and a better affinity than Bis-Bza-Diado ($K_{IE(3)} = 23$ μ M and $K_{IE(BisBzaDiado)} = 129$ μ M). BD6 was found a poor and not selective inhibitor. Both Bis-Bza-Diado and compound **3** were found to be reversible inhibitors, because the MAO activity was completely restored after removal of the inhibitor from enzyme–inhibitor complexes (prepared at 300 μ M of compound concentration), by dilution (data not shown). From data of Table 3, it also appeared that, under our experimental conditions, isatin acts as competitive inhibitor, as previously reported [40], with K_{IE} values of 16 and 2 μ M for MAO A and MAO B, respectively.

These results indicate that the substitution of the diamine chain of **5** with a spermine moiety, affording **3**, transformed a good substrate with high affinity for MAO B in an “inhibitor” (a spermine analogue), selective for MAO B. This behaviour is in agreement with the presence of some polar zones inside MAO B active site (shown also in Fig. 6) and with the described plasticity of the human MAO B active site cavity, which can host both small and cavity-filling ligands, such as safinamide and trans,trans-farnesol [35]. For this reason **3**-structure might be taken into consideration as scaffold to develop novel inhibitors selective for MAO B.

2.2.4. Mode of inhibition of **8** versus MAO A and MAO B

Compound **8** is characterized by a very reactive group, the ITC moiety, so, at first, the possible effect of the incubation time on MAO activity was investigated (experimental details in Section 4.2.4). After incubation with **8**, the activity of MAO A was found to decrease in a time- and concentration-dependent manner, as shown in Fig. 3A. The apparent inactivation rate constant values (k'_{obs}) were determined for each concentration of **8**. The saturation effect showed by the plot of “ k'_{obs} vs **8** concentration” (Fig. 3B) suggested the presence of an equilibrium between the enzyme–**8** complex and the unbound enzyme and unbound **8**, followed by an irreversible step of inactivation of enzyme (Scheme 5, in 4.2.4). Thus, by the best fit of the Kitz–Wilson equation (Eq. (1)) to the data of Fig. 3B, the following kinetic parameters were calculated: $k_{inact} = (3.0 \pm 0.3) \times 10^{-2}$ min⁻¹, $K_{IE} = 5 \pm 1$ μ M and inhibition potency (k_{inact}/K_{IE}) = 6×10^3 M⁻¹ min⁻¹.

No detection of H_2O_2 production was observed during the inactivation reaction that is, no catalytic turnover is necessary to inactivate MAO A with **8**.

The possible effect of **8**-decomposition on its effectiveness in inhibiting MAO A was also evaluated. Compound **8** was pre-incubated in buffer (**8** = 100 μ M, at 30 °C) for 24 h; then, MAO A was added and the inhibitory effectiveness of **8** was determined after 10 min of incubation with the enzyme. After 24 h in buffer, **8**

Table 2
Effect of compounds **1–4** and **8** on kinetic parameters of human VAP-1, MAO A and MAO B, in comparison to Bis-Bza-Diado, BD6 and spermine.

Compound (200 μ M)	VAP-1 (S = BZA) ^a		MAO-A (S = tyramine) ^a		MAO B (S = BZA) ^a	
	Relative V_{max}	Relative V_{max}/K_m	Relative V_{max}	Relative V_{max}/K_m	Relative V_{max}	Relative V_{max}/K_m
Control	1	1	1	1	1	1
Bis-Bza-Diado	0.89 ^b	0.35 ^b	0.52	0.29	0.62 ^b	0.37 ^b
Spermine	1.0	0.96	0.77	0.86	0.98	0.76
BD6	0.77 ^b	0.66 ^b	0.48	0.38	0.97 ^b	0.66 ^b
1	1.12	0.97	0.52	0.62	0.81	0.91
2	0.85	0.69	0.52	0.72	0.93	0.72
3	1.0	0.6	0.52	0.57	0.63	0.05
4	Substrate	Substrate	0.96	0.69	0.71	0.75
8	0.69	0.66	Very low	Very low	Very low	Very low

Kinetic measurements were performed after 30 min of pre-incubation of VAP-1 and MAOs with the potential inhibitor, at 37 and 30 °C, respectively.

^a Kinetic parameters were determined using the following substrates: BZA for VAP-1 and MAO B and tyramine for MAO A. The kinetic parameter values of control samples are those reported in Table 1, footnote “a”.

^b From Bonaiuto et al. [15].

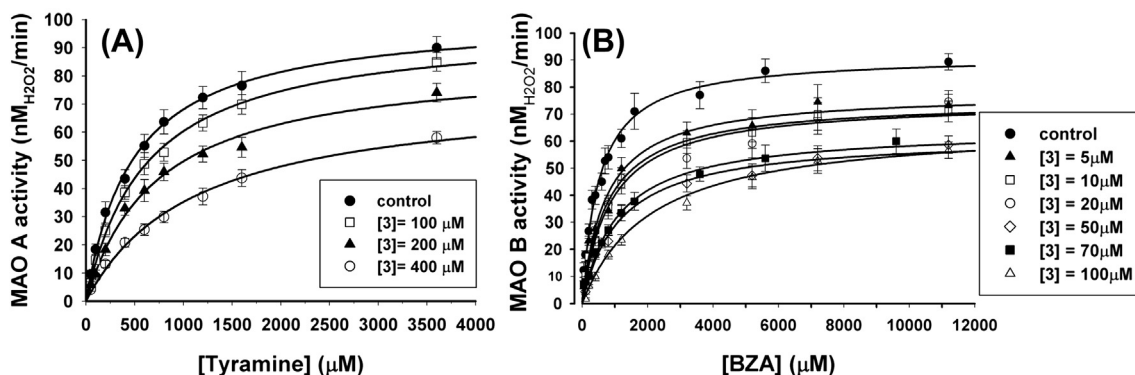


Fig. 2. Effect of compound **3** on monoamine oxidase activity. Plots of initial velocity versus substrate concentration of human recombinant MAO A (panel A) and MAO B (panel B), in the presence of various concentrations of compound **3**. Measurements were performed after 30 min of pre-incubation of the enzyme in the presence or absence of **3**, at 30 °C. Solid lines are the results of the best fitting of the mixed inhibition model to the experimental data.

Table 3

Inhibition constants and mode of inhibition of Bis-Bza-Diado, compounds **3**, **8** and of a reference inhibitor for human recombinant MAOs.

Inhibitor	K_{IE} and (K_{IES}) ^a (μM)		Selectivity $K_{IE,MAO A} / K_{IE,MAO B}$	Type of inhibition	
	MAO A ^a	MAO B ^b		MAO A	MAO B
Bis-Bza-Diado	55 ± 22 (186 ± 100)*	129 ± 20 ^{a,c} (1048 ± 151)* ^c	1:2.3	Mixed, reversible	Mixed, reversible
BD6	170 ± 15 (188 ± 40)*	291 ± 30 (785 ± 161)*	1:1.7	Mixed, reversible	Mixed, reversible
3	226 ± 34 (997 ± 337)*	23 ± 4 (414 ± 97)*	9.8:1	Mixed, reversible	Mixed, reversible
8	5 ± 1	9 ± 2	1:1.8	Irreversible	Competitive
Isatin	16 ± 2	2.0 ± 0.1	8:1	Competitive	Competitive
Clorgyline	0.012 ± 0.001			Irreversible	
Selegiline		0.055 ± 0.018			Irreversible

^a Tyramine was used as substrate.

^b BZA was used as substrate.

^c From Bonaiuto et al., 2012 [15].

lost its inhibitory effect because no enzyme inactivation was observed (100% of residual MAO A activity respect to 64% of residual activity found without pre-incubation of **8** in buffer). This behaviour indicates that **8**, due the ITC moiety, decomposes in water solution to a compound that is not active as inhibitor. Additionally, this by-product did not act as substrate for MAO A, because no hydrogen peroxide generation was detected in the assay solution, in the absence of tyramine (substrate).

To test the reversibility of the inactivation by **8**, MAO A (0.025 mg/ml) was incubated in the presence of **8** (**8** = 200 μM).

When the residual activity was lower than 25%, the sample was extensively dialysed against several changes of buffer (potassium phosphate 50 mM pH 7.40, at 4 °C). A control sample of MAO A was run simultaneously, under the same experimental conditions. After the dialysis, no recovery of MAO activity was detected in the sample previously inactivated with **8**. This result indicates that **8** acts as an irreversible MAO A inhibitor.

The inhibitory behaviour of **8** was compared to that of three known irreversible inhibitors that react with the FAD cofactor: clorgyline and selegiline, the known selective inhibitors for MAO A

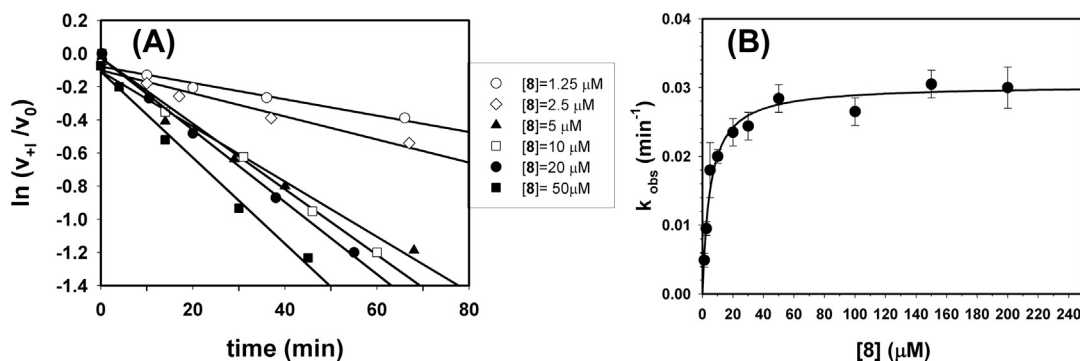


Fig. 3. Mode of inhibition of compound **8** vs MAO A. *Panel A:* time- and concentration dependent MAO A inhibition by **8**. Plots of logarithm of residual MAO A activity respect to control sample versus pre-incubation time with **8**. The concentrations of inhibitor were in the range of 1.25–50 μM; higher concentrations of **8** are not shown because the “saturation effect” gives overlapping plots. Tyramine 1 mM was used as substrate to measure residual enzyme activity. Solid lines were calculated by linear-regression analysis of data; the slope values of each straight line are the apparent inactivation rate constant of MAO A (k'_{obs}) at the given inhibitor concentration. *Panel B:* plot of apparent inactivation rate constant of MAO A (k'_{obs}) by **8**, as a function of inhibitor concentration. Fitting the Kitz–Wilson equation (Eq. (1)) to plotted data (continuous line), an inactivation rate constant $k_{inact} = (3.0 \pm 0.3) \times 10^{-2} \text{ min}^{-1}$ and an inhibition constant $K_{IE} = 5 \pm 1 \text{ μM}$ were calculated.

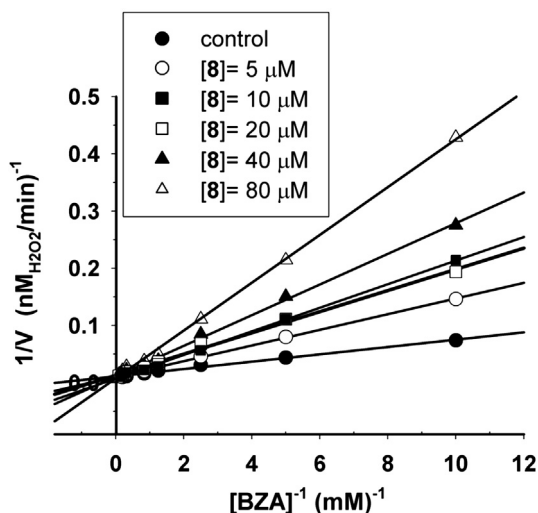


Fig. 4. Mode of inhibition of compound **8** vs MAO B. Lineweaver–Burk plots of initial velocity and substrate concentrations, in the presence of various concentrations of **8**. Benzylamine was used as MAO B substrate. A $K_{IE} = 9 \pm 2 \mu\text{M}$ was calculated according to the competitive inhibition model.

and MAO B respectively (data reported in Table 3), and trans-2-phenylcyclopropylamine, a non-specific AO inhibitor (data not shown). In the case of MAO A, under our experimental conditions, $k_{\text{inact}} = (86 \pm 11) \times 10^{-2} \text{ min}^{-1}$, $K_{IE} = 12.5 \pm 1.0 \text{ nM}$ and inhibition potency (k_{inact}/K_{IE}) = $7 \times 10^7 \text{ M}^{-1} \text{ min}^{-1}$ were determined for clorgyline; $k_{\text{inact}} = 4.0 \pm 0.8 \text{ min}^{-1}$, $K_{IE} = 66 \pm 25 \mu\text{M}$ and inhibition potency (k_{inact}/K_{IE}) = $6 \times 10^4 \text{ M}^{-1} \text{ min}^{-1}$ were obtained for trans-2-phenylcyclopropylamine, in agreement with previously reported data [41]. In the case of MAO B and selegiline, $k_{\text{inact}} = (80 \pm 5) \times 10^{-3} \text{ min}^{-1}$ and $K_{IE} = 55 \pm 18 \text{ nM min}^{-1}$ were obtained.

The results above reported indicate that **8**, even if less potent than clorgyline, may represent a novel type of irreversible MAO A inhibitor, thanks to its ITC group, a novel reactive moiety for MAO A.

Differently to MAO A, **8** was found to act as competitive inhibitor of MAO B, with $K_{IE} = 9 \pm 2 \mu\text{M}$, as clearly shown by the Lineweaver–Burk plots of Fig. 4; no time-dependent inactivation of MAO B activity by **8** was observed, testing **8** at the maximum concentration of $100 \mu\text{M}$. This different mode of inhibition of **8** for the two MAO isoforms, irreversible for MAO A and competitive for MAO B is very

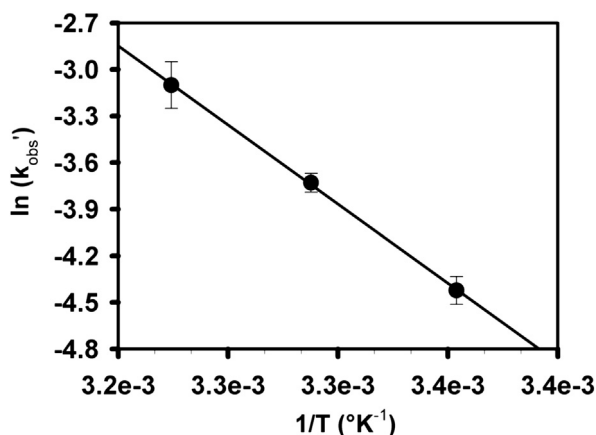


Fig. 5. Effect of temperature on inactivation rate constant of MAO A by **8**. Arrhenius plot of apparent inactivation rate constant (k_{obs} , in min^{-1}) of MAO A by **8**, at $50 \mu\text{M}$ of inhibitor concentration. Tyramine (1 mM) was used as substrate. From the slope of the linear regression to the kinetic data, activation energy of 20.2 kcal/mol was calculated.

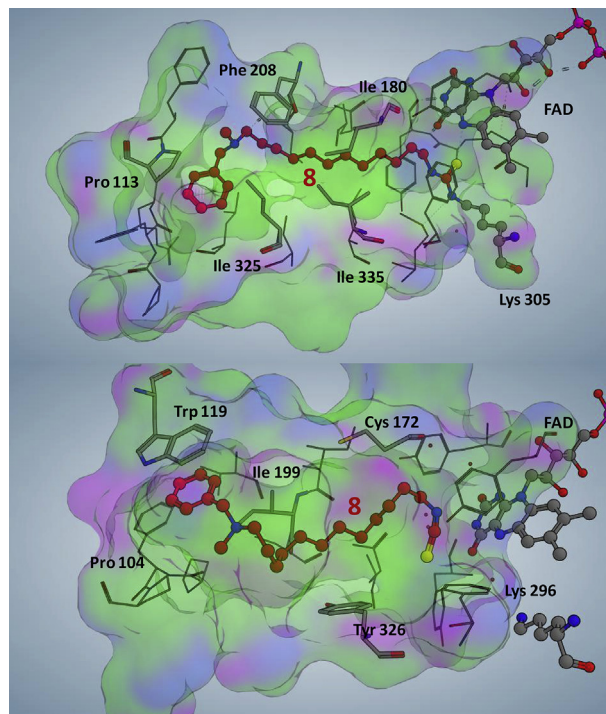


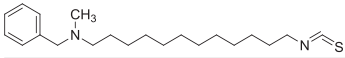
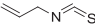
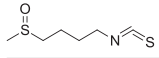
Fig. 6. Interaction models of **8** into MAO active site. Panel A: Possible irreversible interaction model of **8** (red) inside MAO A active site, after the molecular docking and the Molecular Dynamics procedures. Panel B: docking pose of **8** (red) inside MAO B. MAO A and MAO B molecular surfaces are also highlighted: green for hydrophobic zones, blue/violet for polar aminoacids. (For interpretation of the references to colour in this figure legend, the reader is referred to the web version of this article.)

interesting for potential pharmacological development. Other types of inhibitors have already shown a different mode of inhibition for the two enzyme isoforms: mofegiline, for example, acts as an irreversible inhibitor of MAO B and reversible of MAO A [42].

2.2.5. **8** versus MAOs from human adipocytes lysates

The effect of **8** was tested on the native MAOs, using lysates from human adipocytes as source of enzyme. The time-dependent inactivation of MAOs was evaluated, by determining the residual MAO activity after various periods of pre-incubation of lysate with $50 \mu\text{M}$ of compound **8** (Fig. S2 in Supplementary information): an apparent inactivation rate constant (k'_{obs}) $\approx 13 \times 10^{-3} \text{ min}^{-1}$ was calculated, that raises to about (k'_{obs}) $\approx 20 \times 10^{-3} \text{ min}^{-1}$, if the contribute in MAO B activity (29%, determined as reported in Section 4.2.1) to the total MAO activity was taken into account and supposed do not decay, as found for the recombinant enzyme (MAO B). These values, even if lower than that determined using the recombinant enzyme ($k'_{\text{obs}} \approx 25 \times 10^{-3} \text{ min}^{-1}$), indicate that **8** is able to inactivate also the native enzyme present in a raw sample. Additionally, to evaluate the inhibition constant of **8** for the native MAOs, the kinetic parameters of MAO activity of adipocytes were determined in the presence of **8** ($6\text{--}25 \mu\text{M}$), after 5 min of pre-incubation with lysates (0.09 mg/ml in the assay buffer and 0.05% final Triton X-100 concentration). These experimental conditions, short pre-incubation time and low **8** concentrations, allowed these experiments to be performed by normal steady-state approach, with negligible amount of inactivated enzyme respect to total MAOs of samples. A competitive inhibition model was found to give the best fit to the kinetic data (Fig. S3, in Supplementary information) and an inhibition constant, $K_{IE} = 4.9 \pm 0.4 \mu\text{M}$ was calculated; this value is very similar with that found using the

Table 4
Effect of compound **8** in comparison to AITC and sulforaphane on recombinant MAO activity^a.

Enzyme	8 (20 μ M)		AITC (20 μ M)		Sulforaphane (20 μ M)	
						
	Residual V_{\max}	Residual V_{\max}/K_m	Residual V_{\max}	Residual V_{\max}/K_m	Residual V_{\max}	Residual V_{\max}/K_m
MAO A	0.70	0.22	1.0	1.0	0.92	0.78
MAO B	1.01	0.20	1	0.98	0.99	1.01

^a Kinetic parameters were determined after 10 min of pre-incubation of MAOs with the compound at $T = 30^\circ\text{C}$; BZA and tyramine were used as MAO B and MAO A substrate, respectively.

recombinant enzymes (5 and 9 μM for MAO A and B respectively, Table 3).

All these behaviours, time dependent inactivation, K_{IE} values, and competition for substrate binding site confirm the effectiveness of **8** on native human MAOs.

2.2.6. Effect of temperature on MAO A inactivation by **8**

The inactivation of the recombinant MAO A by **8** was determined at various temperatures (25, 30 and 37°C), at 50 μM concentration of inhibitor. The apparent inactivation rate constant values (k'_{obs}), were found to increase with temperature, ranging from about 0.012 min^{-1} , at 25°C , to about 0.045 min^{-1} , at 37°C (physiological temperature). The inactivation of control samples was found slow in comparison to that of samples incubated with compound **8**, that is about 0.004 min^{-1} at 37°C . The plot reported in Fig. 5 shows a linear dependence of logarithm of k'_{obs} versus $1/T$; thus, applying the Arrhenius law, an activation energy of 20.2 kcal/mol was calculated for the reaction of inactivation of MAO A by **8**. This value is quite similar to those calculated for the irreversible inactivation of MAO B by other irreversible inhibitors, rasagiline and selegiline [43].

2.2.7. Effect of other ITC-containing compounds on MAO activity

The effect of **8** on MAO activity was compared to that of other two compounds bearing an ITC moiety: AITC and sulforaphane. The kinetic parameters were determined after 10 min of pre-incubation time of the recombinant enzyme (MAO A or MAO B) in the presence of one of the ITC compounds (at 20 μM concentration). The residual V_{\max} and V_{\max}/K_m values, reported in Table 4, indicate that neither AITC nor sulforaphane have significant effect on MAO V_{\max} in comparison to **8** and only sulforaphane and **8** decrease catalytic efficiency values of MAO A. As for **8**, the possible time-dependent inactivation of MAO A after incubation with sulforaphane was considered. In the presence of 50 μM sulforaphane, an apparent inactivation rate constant (k'_{obs}) $\approx 2 \times 10^{-3}\text{ min}^{-1}$ was calculated; this value is one order of magnitude lower than that determined in the presence of 50 μM of **8** ($k'_{\text{obs}} \approx 25 \times 10^{-3}\text{ min}^{-1}$), under the same experimental conditions. On this basis, we may deduce that sulforaphane can interact with MAO A, but it is not as efficient as **8** in inactivating this enzyme, confirming the important role of the polyamine skeleton in addressing the ITC moiety to MAO A active site.

2.3. Docking studies of **8** and **3** into MAO active site

Docking experiments, followed by Molecular Dynamic (MD) simulation, showed that the compound **8** interacted with MAO A in its catalytic binding site, locating the ITC group close to the Lys 305 (less than 1 Å), an important residue for the catalytic activity; curiously this basic residue is the only basic amino acid present inside the MAO A binding site. In this condition, the distance between the ITC and the Lys 305 amino group is compatible with their

reaction and generation of an thiourea/isothiourea derivative, through the formation of a covalent bond. This event should “anchor” **8** inside the active site cavity preventing the access of the substrate. On the other hand the polymethylene chain of **8**, as well as the phenyl ring, fill the entire binding site making hydrophobic contacts with a large number of residues (Leu 97, Phe 108, Pro 113, Ile 180, Phe 208, Val 210, Ile 335, Ile 325, Leu 337, Met 350, Phe 352). The model described in Fig. 6A could explain the irreversible mechanism of action of **8**.

The same Lysine (Lys 305) is conserved also in MAO B (Lys 296), but in this isoform the aminoacid substitutions of Phe 208 (in MAO A) with Ile 199 (in MAO B) and of Ile 335 (in MAO A) with the bulkier residue Tyr 326 (in MAO B), forced the compound to address the ITC group in a different position, far from Lys 296 (6.83 Å), thus interacting with a cluster of water molecules located close to the FAD (Fig. 6B). Interestingly the binding mode of **8** in MAO B is partially superposed to the one of the MAO B inhibitor pioglitazone (PDB code: 4A79, Fig. S4, see Supplementary information) and is compatible with a reversible mechanism of action.

These docking results, pointing to Lys 305 (in MAO A active site), as possible target of the ITC functional group of **8**, are in good agreement with previous site-directed mutagenic studies which highlighted a role of this conserved Lys in the catalytic mechanism of MAOs. Indeed, human MAO A K305A, MAO B K296A [44], K296R and K296Q [45] mutants have very low or no detectable enzyme activity. From structural studies, the ϵ -amino group of this Lys is H-bonded to N(5) of the flavin ring via a water molecule to form a structural motif that is conserved in the active site of several flavoenzymes [35,46]. Some studies have suggested a possible role of this residue in the O_2 activation to form H_2O_2 [45,47,48].

Thus, **8** might be considered a novel type of MAO inhibitor able to interact covalently with Lys 305 residue inside MAO A active site, involved in the catalytic mechanism of MAOs.

This proposed mechanism is new with respect to the mechanism of inactivation of most irreversible inhibitors, such as clorgyline, which reacts with the cofactor FAD via the classical function propargylamine [35].

Other docking experiments were performed to understand why compound **3** behaved as a more potent inhibitor for MAO B ($K_{IE} = 23\text{ }\mu\text{M}$) respect to MAO A and why BD6 was a poor inhibitor for both MAO isoforms (inhibition constant value around 200 μM).

Results showed that BD6 and compound **3** accommodated similarly inside MAO B binding cleft, in particular locating their hydrophobic rings in a small cleft surrounded by Trp119, Phe103, Ile 199, Pro 104 (data not shown). The *in silico* analysis suggests that a six atoms ring (BD6) displays much more steric clashes than the five atoms ring (compound **3**), and this may be responsible for the better inhibitory potency of compound **3** respect to BD6. On the other hand in MAO A both BD6 and compound **3** cannot target a similar binding cleft due to a different configuration of the residues in MAO A binding site, leading to the poor inhibition potency for both molecules shown by the kinetic approach.

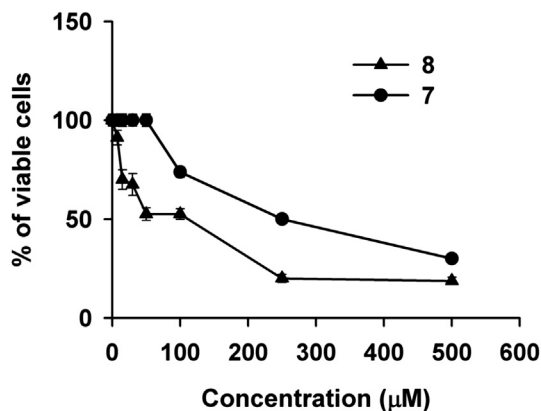


Fig. 7. Cytotoxicity of compounds **7** and **8**, against SH-SY5Y cells after 24 h of compound exposure. Data are means \pm SEM of at least three independent experiments.

2.4. Biological evaluation: cytotoxic activity in vitro of compound **7** and **8**

Compounds **7** and **8** were evaluated for their cytotoxic effects by *in vitro* assays on human dopaminergic neuroblastoma SH-SY5Y cells (Fig. 7). Compound **7**, bearing a primary amino group instead of the ITC moiety of **8**, was included in the study as precursor of **8**. Fig. 6 shows the growth curve of SH-SY5Y cells after treatment with different concentrations of **7** or **8**. When the harvested cells were counted, the numbers of control cells continued to increase, whereas the numbers of treated cells decreased in a dose-dependent manner. The IC_{50} , as measured by the number of viable cells in cultures 24 h after the addition of **7** or **8**, was seen at a concentration of about 327 μ M and 180 μ M for **7** and **8**, respectively. The cytotoxic activity of sulforaphane against SH-SY5Y cells (IC_{50} values of 20 μ M) [28] is higher than that of **8**, indicating that **8**-scaffold may be taken into account for future development of novel MAOs inhibitors endowed with very low cytotoxic activity.

3. Conclusion

The main findings here reported suggest that a polyamine skeleton, suitably modified, has given rise to the development both of substrates and of novel type of MAO inhibitors. In particular, two new types of MAO inhibitors, selective respect to VAP-1, emerged in this study: the spermine analogue **3**, bearing a thiophene ring, which acts as mixed reversible inhibitor ($K_i = 23 \mu$ M), selective for MAO B; and compound **8**, obtained by transforming the primary amine function of very good AOs substrates like **7** and **24**, in an ITC moiety. **8** shows high affinity for both MAO isoforms (K_i about 5–10 μ M), but it acts as competitive inhibitor of MAO B and as irreversible inhibitor of MAO A. As resulting by the docking studies, Lys 305 of the MAO A active site has been proposed as a new target for covalently binding the ITC reactive moiety of **8**, leading to MAO A irreversible inhibition. At present we are not able to definitively exclude other mechanisms of interactions of **8** with MAO A, for example with FAD or with the thiol groups of Cys 321 and Cys 323 located close to the entrance of the MAO A active site cavity [49]; further studies will be necessary to confirm the results of the docking studies.

In conclusion, for the first time we gathered evidence that an ITC group, mounted on an appropriate scaffold, led to inactivation of MAO A and may be used as a probe to identify one of the possible mechanism of MAO A inhibition.

Studies are in progress to modify the structure of the compound **8** for improving its interaction with MAOs, mainly in physiologic

conditions (at 37 °C), and to evaluate its interaction with other amino oxidases, such as polyamine oxidases.

Further studies will be needed to evaluate the ability of the compounds of the present study to reach the central nervous system and consequently their potential in developing novel therapies for pathologies involving MAOs. In this regard, we recently found that polyamines endowed with similar features are able to cross the blood brain barrier [50].

As future perspective, the study aims to use these novel molecules (compounds **3** and **8**) alone, or in combination with the system “copper-amine oxidases/polyamines” [51] to investigate more in depth the biological effect on cellular systems. It might represent a new approach in therapy.

4. Experimental section

4.1. Chemistry

All the synthesized compounds **1–8** have a purity of at least 95% determined by elemental analysis. The elemental analysis was performed with Perkin Elmer elemental analyzer 2400 CHN. Melting points were taken in glass capillary tubes on a Buchi SMP-20 apparatus and are uncorrected. 1H and ^{13}C NMR spectra were recorded on Varian VXR 400 and 200 spectrometer in $CDCl_3$, CD_3OD or D_2O as solvents. Chemical shifts are given in ppm, J values are given in Hz, and spin multiplicities are given as s (singlet), brs (broad singlet), d (doublet), t (triplet), q (quartet), or m (multiplet). Electron spray ionization (ESI) mass spectra were recorded on VG 7070E instrument. Chromatographic separations were performed on silica gel columns by flash (Kieselgel 40, 0.040–0.063 mm; Merck), or gravity column (Kieselgel 60, 0.063–0.200 mm; Merck) chromatography. Reactions were followed by thin-layer chromatography (TLC) on Merck (0.25 mm) glass-packed precoated silica gel plates (60 F254) that were visualized in an iodine chamber, UV lamp and bromocresol green. The term “dried” refers to the use of anhydrous sodium sulphate.

4.1.1. General procedure for the synthesis of **9–11**

A solution of tri-Boc-spermine (0.502 g, 1 mmol) and the appropriate aldehyde (1.1 mmol) in toluene (50 ml) was refluxed in a Dean–Stark apparatus for 3 h and on cooling solvent was removed in vacuo. $NaBH_4$ (0.151 g, 4 mmol) was added to a cooled (0 °C) solution of the residue in EtOH (30 ml) and stirring was continued at room temperature for 4 h. The solvent was then removed and the residue was dissolved in CH_2Cl_2 (30 ml) and washed with H_2O (3 \times 20 ml). Removal of the dried solvent in vacuo gave a residue that was purified by flash chromatography eluting with CH_2Cl_2 /MeOH/33% aq. NH_4OH (9:1:0.05).

4.1.2. *tert*-Butyl(4-((*tert*-butoxycarbonyl)(3-((*tert*-butoxycarbonyl)amino)propyl)amino)butyl)(3-((naphthalen-2-ylmethyl)amino)propyl)carbamate (**9**)

Yellow oil; 81% yield; 1H NMR ($CDCl_3$, 400 MHz) δ 1.39–1.42 (m, 29H + 1H exch with D_2O), 1.61–1.73 (m, 4H), 2.63 (t, $J = 6.8$ Hz, 2H) 3.05–3.20 (m, 12H), 3.92 (s, 2H), 5.25 (brs, 1H exch with D_2O), 7.12–7.14 (m, 1H), 7.42–7.45 (m, 3H), 7.73–7.79 (m, 3H).

4.1.3. *tert*-Butyl(4-((*tert*-butoxycarbonyl)(3-((*tert*-butoxycarbonyl)amino)propyl)amino)butyl)(3-((pyridin-3-ylmethyl)amino)propyl)carbamate (**10**)

Yellow oil; 84% yield; 1H NMR ($CDCl_3$, 200 MHz) δ 1.44–1.49 (m, 29H), 1.68–1.75 (m, 4H), 2.04 (brs, 1H exch with D_2O), 2.61 (t, $J = 6.8$ Hz, 2H), 3.08–3.24 (m, 12H), 3.79 (s, 2H), 5.33 (brs, 1H exch with D_2O), 7.16–7.32 (m, 2H), 7.67–7.75 (m, 1H), 8.48–8.60 (m, 1H).

4.1.4. *tert*-Butyl(4-((*tert*-butoxycarbonyl)(3-((*tert*-butoxycarbonyl)amino)propyl)amino)butyl)(3-((thiophen-2-ylmethyl)amino)propyl)carbamate (**11**)

Yellow oil; 90% yield; ^1H NMR (CDCl_3 , 200 MHz) δ 1.35–1.47 (29H + 1H exch with D_2O), 1.65–1.75 (m, 4H), 2.63 (t, J = 6.8 Hz, 2H), 3.08–3.24 (m, 12H), 3.96 (s, 2H), 5.29 (brs, 1H exch with D_2O), 6.94–7.00 (m, 2H), 7.23–7.30 (m, 1H).

4.1.5. General procedure for the synthesis of **1–3**

A solution of the appropriate compounds **9–11** (0.7 mmol) in 30 ml of MeOH and 20 ml of aq. HCl 3 M (10 ml) was stirred overnight at room temperature. Following solvent removal, the residue was washed with Et_2O (5×20 ml). The resulting solid was filtered and dried to afford the corresponding tetrahydrochloride salt as a white solid.

4.1.6. N^1 -(3-Aminopropyl)- N^4 -(3-((naphthalen-2-ylmethyl)amino)propyl)butane-1,4-diamine (**1**)

White solid; quantitative yield; mp > 250 °C; ^1H NMR (D_2O , 200 MHz) δ 1.62–1.66 (m, 4H), 1.93–2.05 (m, 4H), 2.94–3.14 (m, 12H), 4.31 (s, 2H), 7.42–7.54 (m, 3H), 7.85–7.93 (m, 4H); ^{13}C NMR (D_2O , 100 MHz) δ 22.6, 22.7, 23.7, 36.5, 43.9, 44.4, 44.5, 46.9, 51.2, 51.3, 126.5, 127.0, 127.7, 127.9, 128.0, 129.7, 129.8, 130.3, 132.7, 133.1; MS (ESI^+) m/z = 172 ($\text{M} + 2\text{H}$) $^{2+}$.

4.1.7. N^1 -(3-Aminopropyl)- N^4 -(3-((pyridin-3-ylmethyl)amino)propyl)butane-1,4-diamine (**2**)

White solid, quantitative yield, mp > 250 °C, ^1H NMR (D_2O , 400 MHz) δ 1.64–1.68 (m, 4H), 1.92–2.07 (m, 4H), 2.95–3.07 (m, 10H), 3.18 (t, J = 7.8 Hz, 2H), 4.43 (s, 2H), 8.01 (t, J = 7.0 Hz, 1H), 8.58 (d, J = 6.8 Hz, 1H), 8.76 (d, J = 5.6 Hz, 1H), 8.84 (s, 1H); ^{13}C NMR (D_2O , 100 MHz) δ 22.6, 22.7, 23.7, 36.5, 44.3, 44.5, 44.7, 46.9, 47.0, 48.7, 48.8, 127.1, 127.7, 130.8, 142.9, 147.7; MS (ESI^+) m/z = 148 ($\text{M} + 2\text{H}$) $^{2+}$.

4.1.8. N^1 -(3-Aminopropyl)- N^4 -(3-((thiophen-2-ylmethyl)amino)propyl)butane-1,4-diamine (**3**)

White solid; quantitative yield; mp > 250 °C; ^1H NMR (D_2O , 400 MHz) δ 1.80 (m, 4H), 2.09–2.15 (m, 4H), 3.11–3.23 (m, 12H), 4.53 (s, 2H), 7.15–7.16 (m, 1H), 7.31–7.32 (m, 1H), 7.59–7.60 (m, 1H); ^{13}C NMR (D_2O , 100 MHz) δ 22.54, 22.68, 23.67, 36.48, 43.38, 44.40, 44.47, 44.95, 46.93, 127.82, 128.77, 131.01, 131.06; MS (ESI^+) m/z = 150 ($\text{M} + 2\text{H}$) $^{2+}$.

4.1.9. 3-(2,2,2-Trifluoroacetamido)propyl 4-methylbenzenesulfonate (**13**)

To a stirred and cooled (0 °C) solution of **12** [30] (2.87 g, 16.8 mmol) and Et_3N (3.5 ml, 25.2 mmol) in dry CH_2Cl_2 (25 ml) was added tosyl chloride (3.51 g, 18.4 mmol) in dry CH_2Cl_2 (10 ml) within 10 min. Stirring was continued for 1 h at 0 °C and then overnight at room temperature. The reaction mixture was washed with 1 M NaHCO_3 solution (3×40 ml). The organic phase was dried, evaporated in vacuo and the residue was purified by flash chromatography eluting with a mixture of petroleum ether/ethyl acetate (3:1) to give **13** as a yellow oil: 58% yield; ^1H NMR (CDCl_3 , 400 MHz) δ 1.94–1.99 (m, 2H), 2.46 (s, 3H), 3.45–3.50 (m, 2H), 4.11 (t, J = 5.6 Hz, 2H), 6.67 (brs, 1H exch with D_2O), 7.37 (d, J = 6.0 Hz, 2H), 7.79 (d, J = 6.4 Hz, 2H).

4.1.10. *tert*-Butyl (8-((3-(2,2,2-trifluoroacetamido)propyl)amino)octyl)carbamate (**15**)

To a stirred solution of **13** (1.5 g, 4.6 mmol) in THF (25 ml) was added **14** [31] (1.12 g, 4.6 mmol) in one portion and the resulting mixture was reflux for 4 h. The solvent was evaporated in vacuo and the residue was purified by flash chromatography eluting with a mixture of toluene/ CH_2Cl_2 /MeOH/33% aq. NH_4OH (5:4:1:0.05) to

give **15** as yellow oil: 41% yield; ^1H NMR (CDCl_3 , 400 MHz) 1.25 (s, 9H), 1.40–1.47 (m, 10H + 1H exch with D_2O), 1.52–1.55 (m, 4H), 2.71 (t, J = 8.0 Hz, 2H), 2.91 (t, J = 5.6 Hz, 2H), 3.08–3.09 (m, 2H), 3.47 (t, J = 7.2 Hz, 2H), 4.55 (brs, 1H exch with D_2O), 5.67 (brs, 1H exch with D_2O); ^{13}C NMR (CDCl_3 , 100 MHz) δ 21.2, 25.7, 26.6, 27.8, 28.4, 28.9, 29.6, 38.8, 40.5, 47.3, 49.0, 50.4, 78.9, 112.0, 114.5, 117.4, 120.0, 156.0, 157.1, 157.3, 157.7, 157.9.

4.1.11. *tert*-Butyl (8-((3-aminopropyl)amino)octyl)carbamate (**16**)

To a stirred solution of **15** (0.60 g, 1.5 mmol) in MeOH, a NaOH 40% solution (1.7 ml) was added. The resulting mixture was stirred at room temperature overnight. The solvent was removed in vacuo and the resulting residue was taken up with CHCl_3 (20 ml) and washed with brine (20 ml \times 4) to furnish **16** as yellow oil; quantitative yield; ^1H NMR (CDCl_3 , 400 MHz) δ 1.29 (s, 9H), 1.44–1.50 (m, 12H + 3H exch with D_2O) 1.61–1.67 (m, 2H), 2.59 (t, J = 7.6 Hz, 2H), 2.67 (t, J = 7.2 Hz, 2H), 2.77 (t, J = 6.8 Hz, 2H), 3.09–3.11 (m, 2H), 4.64 (brs, 1H exch with D_2O); ^{13}C NMR (CDCl_3 , 100 MHz) δ 26.2, 26.8, 27.1, 27.9, 28.7, 28.9, 29.1, 29.5, 33.2, 40.0, 47.4, 49.6, 78.0, 155.6.

4.1.12. *tert*-Butyl (8-((3-((thiophen-2-ylmethyl)amino)propyl)amino)octyl)carbamate (**17**)

A solution of **16** (0.13 g, 0.43 mmol) and 2-thiophenecarbaldehyde (0.058 g, 0.52 mmol) in toluene (10 ml) was stirred at the refluxing temperature in a Dean–Stark apparatus for 3 h. After cooling, the solvent was evaporated, and the residue was dissolved in EtOH (10 ml), cooled in an ice bath, and treated with NaBH_4 (0.02 g, 0.52 mmol); the reaction mixture was stirred 4 h at room temperature. The solvent was then removed and the residue was dissolved in CH_2Cl_2 (30 ml) and washed with H_2O (3×20 ml). Removal of the dried solvent in vacuo gave a residue that was purified by flash chromatography eluting with a mixture of toluene/ CH_2Cl_2 /MeOH/33% aq. NH_4OH (5:4:1:0.05) to give **17** as yellow oil: 77% yield; ^1H NMR (CD_3OD , 400 MHz) δ 1.25–1.40 (m, 19H), 1.58–1.65 (m, 2H), 2.01–2.09 (m, 2H), 2.90–2.93 (m, 4H), 3.02 (t, J = 8.0 Hz, 2H), 3.09 (t, J = 7.6 Hz, 2H), 4.39 (s, 2H), 7.01–7.03 (m, 1H), 7.25–7.27 (m, 1H), 7.47–7.48 (m, 1H).

4.1.13. N^1 -(3-((Thiophen-2-ylmethyl)amino)propyl)octane-1,8-diamine (**4**)

A solution of **17** (0.130 g, 0.33 mmol) in MeOH (10 ml) and HCl 3 M (10 ml) was stirred overnight at room temperature. Following solvent removal, the residue was washed with Et_2O (5×20 ml). The resulting solid was filtered and dried to afford **4** as trihydrochloride salt; white solid; quantitative yield; mp > 250 °C; ^1H NMR (D_2O , 400 MHz) δ 1.20–1.24 (m, 8H), 1.49–1.54 (m, 4H), 1.95–1.99 (m, 2H), 2.84 (t, J = 7.6 Hz, 2H), 2.90 (t, J = 7.6 Hz, 2H), 2.98 (t, J = 8.0 Hz, 2H), 3.05 (t, J = 8.0 Hz, 2H), 4.37 (s, 2H), 6.98–7.01 (m, 1H), 7.15–7.17 (m, 1H), 7.43–7.5 (m, 1H); ^{13}C NMR (D_2O , 100 MHz) δ 22.5, 25.4, 25.5, 26.6, 27.9, 39.4, 43.4, 44.2, 44.9, 47.8, 127.8, 128.8, 131.0, 131.1; MS (ESI^+) m/z = 150 ($\text{M} + 2\text{H}$) $^{2+}$.

4.1.14. *tert*-Butyl (12-((thiophen-2-ylmethyl)amino)dodecyl)carbamate (**20**)

A solution of **18** [31] (0.16 g, 0.53 mmol) and 2-thiophenecarbaldehyde (0.060 g, 0.47 mmol) in toluene (10 ml) was stirred at the refluxing temperature in a Dean–Stark apparatus for 3 h. After cooling, the solvent was evaporated, and the residue was dissolved in EtOH (10 ml), cooled in an ice bath, and treated with NaBH_4 (0.02 g, 0.52 mmol); the reaction mixture was stirred 4 h at room temperature. The solvent was then removed and the residue was dissolved in DCM (20 ml) and washed with H_2O (3×20 ml). Removal of the dried solvent in vacuo gave a residue that was purified by flash chromatography with a mixture of

petroleum ether/CH₂Cl₂/MeOH/33% aq. NH₄OH (5:4:1:0.02) to give **20** as yellow oil: 70% yield; ¹H NMR (CDCl₃, 400 MHz) δ 1.20–1.27 (m, 18H + 1H exch with D₂O), 1.44 (s, 9H), 1.53–1.61 (m, 2H), 2.69 (t, J = 7.2 Hz, 2H), 3.07–3.12 (m, 2H), 4.01 (s, 2H), 4.49 (brs, 1H exch with D₂O), 6.96–6.99 (m, 1H), 7.01–7.03 (m, 1H), 7.22–7.29 (m, 1H). ¹³C NMR (CDCl₃, 100 MHz) δ 26.8, 27.1, 28.4, 28.8, 29.2, 29.3, 29.5, 30.0, 40.6, 47.2, 48.2, 59.5, 78.9, 125.0, 125.1, 126.5, 126.9, 156.0.

4.1.15. *N*¹-(Thiophen-2-ylmethyl)dodecane-1,12-diamine (**5**)

A solution of **20** (0.090 g, 0.22 mmol) in MeOH (10 ml) and HCl 3 M (10 ml) was stirred overnight at room temperature. Following solvent removal, the residue was washed with Et₂O (5 \times 20 ml). The resulting solid was filtered and dried to afford **5** as dihydrochloride salt; white solid; quantitative yield; mp > 250 °C; ¹H NMR (D₂O, 400 MHz) δ 1.14–1.21 (m, 16H), 1.49–1.55 (m, 4H), 2.84 (t, J = 7.6 Hz, 2H), 2.92 (t, J = 8.0 Hz, 2H), 4.32 (s, 2H), 6.98–7.07 (m, 1H), 7.11–7.15 (m, 1H), 7.42 (d, J = 5.2 Hz, 1H); ¹³C NMR (CDCl₃, 50 MHz) δ 21.0, 26.0, 28.0, 29.3, 29.4, 38.2, 46.2, 47.9, 68.6, 68.9, 70.2, 70.3, 78.2, 123.8, 124.4, 126.1, 127.8; MS (ESI⁺) m/z = 297 (M + 1H)⁺

4.1.16. *tert*-Butyl (3-(4-(3-((thiophen-2-ylmethyl)amino)propoxy)butoxy)propyl)carbamate (**21**)

A solution of **19** [32] (0.41 g, 1.34 mmol) and 2-thiophenecarbaldehyde (0.181 g, 1.62 mmol) in toluene (10 ml) was stirred at the refluxing temperature in a Dean–Stark apparatus for 3 h. After cooling, the solvent was evaporated, and the residue was dissolved in EtOH (10 ml), cooled in an ice bath, and treated with NaBH₄ (0.061 g, 1.62 mmol); the reaction mixture was stirred 4 h at room temperature. The solvent was then removed and the residue was dissolved in CH₂Cl₂ (20 ml) and washed with H₂O (3 \times 20 ml). Removal of the dried solvent in vacuo gave a residue that was purified by flash chromatography with a mixture of petroleum ether/CH₂Cl₂/MeOH/33% aq. NH₄OH (5:4:1:0.02) to give **21** as yellow oil: 59% yield; ¹H NMR (CDCl₃, 200 MHz) δ 1.45 (s, 9H), 1.62–1.74 (m, 8H), 1.97 (brs, 1H exch with D₂O), 2.75 (t, J = 7.0 Hz, 2H), 3.17–3.16 (m, 2H), 3.4–3.52 (m, 8H), 3.98 (s, 2H), 4.99 (brs, 1H exch with D₂O), 6.92–6.98 (m, 2H), 7.18–7.24 (m, 1H); ¹³C NMR (CDCl₃, 50 MHz) δ 21.0, 26.0, 28.0, 29.3, 29.4, 38.2, 46.2, 47.9, 68.6, 68.9, 70.2, 70.3, 78.2, 123.8, 124.4, 126.1, 143.7, 155.6.

4.1.17. 3-(4-(3-Aminopropoxy)butoxy)-*N*-(thiophen-2-ylmethyl)propan-1-amine (**6**)

A solution **21** (0.320 g, 0.80 mmol) in MeOH (20 ml) and HCl 3 M (20 ml) was stirred overnight at room temperature. Following solvent removal, the residue was washed with Et₂O (5 \times 20 ml). The resulting solid was filtered and dried to afford **6** as dihydrochloride salt; white solid; quantitative yield; mp > 250 °C; ¹H NMR (D₂O, 400 MHz) δ 1.39–1.45 (m, 4H), 1.76–1.86 (m, 4H), 2.94 (t, J = 7.2 Hz, 2H), 3.03 (t, J = 7.6 Hz, 2H), 3.34–3.46 (m, 8H), 4.44 (s, 2H), 6.98–7.00 (m, 1H), 7.14–7.16 (m, 1H), 7.41–7.43 (m, 1H); ¹³C NMR (D₂O, 100 MHz) δ 25.2, 25.3, 26.5, 37.4, 44.6, 44.8, 67.5, 70.4, 70.4, 127.8, 128.6, 130.9, 131.4; MS (ESI⁺) m/z = 301 (M + 1H)⁺.

4.1.18. *N*¹-Benzylododecane-1,12-diamine (**7**)

7 was synthesized as previously reported for Bis-Bza-Diado [15] using a 1:1 mol ratio of 1,12-diaminododecane and benzaldehyde; mp > 250 °C; ¹H NMR (D₂O, 400 MHz) δ 1.14–1.21 (m, 16H), 1.47–1.58 (m, 4H), 2.84 (t, J = 7.6 Hz, 2H), 2.91 (t, J = 8.0 Hz, 2H), 4.09 (s, 2H), 7.33–7.37 (m, 5H); ¹³C NMR (D₂O, 100 MHz) δ 25.3, 25.5, 25.6, 26.6, 28.0, 28.1, 28.3, 28.4, 28.5, 39.5, 46.9, 50.8, 129.2, 129.5, 129.7, 130.7; MS (ESI⁺) m/z = 291 (M + 1H)⁺.

4.1.19. *N*-(12-(Benzylamino)dodecyl)-2,2,2-trifluoroacetamide (**22**)

Ethyl trifluoroacetate (0.074 g, 0.52 mmol) in MeOH (50 ml) was added to a solution of **7** (0.150 g, 0.52 mmol) in MeOH (500 ml)

at –78 °C for 1 h. After stirring for an additional 1 h, the mixture was allowed to reach slowly room temperature and stirred overnight. The solvent was removed and the residue was purified by flash-chromatography eluting with a mixture of CH₂Cl₂/MeOH/33% aq. NH₄OH (9:1:0.05) to give **22** as yellow oil: 86% yield; ¹H NMR (CDCl₃, 200 MHz) δ 1.28–1.53 (m, 20H + 3H exch with D₂O), 2.62–2.73 (m, 2H), 3.65 (t, J = 6.6 Hz, 2H), 3.81 (s, 2H), 7.28–7.35 (m, 4H).

4.1.20. *N*-(12-(Benzyl(methyl)amino)dodecyl)-2,2,2-trifluoroacetamide (**23**)

A solution of **22** (0.250 g, 0.63 mmol) in 85% formic acid (3.7 ml) and 40% formaldehyde (3.7 ml) was refluxed for 24 h. The solution was cooled down, made basic to pH 8 with KHSO₄ and extracted with CHCl₃ (3 \times 30 ml); the organic solvent was dried and removed in vacuo to give **23** as yellow oil: 93% yield; ¹H NMR (CDCl₃, 200 MHz) δ 1.04–1.16 (m, 16H), 1.37–1.44 (m, 2H), 1.46–1.63 (m, 2H), 2.51 (s, 3H), 2.75–2.79 (m, 2H), 3.10–3.20 (m, 2H), 4.03 (s, 2H), 4.90 (brs, 1H exch with D₂O), 7.33–7.37 (m, 4H), 7.77–7.83 (m, 1H).

4.1.21. *N*¹-Benzyl-*N*¹-methylododecane-1,12-diamine (**24**)

To a solution of **23** (0.24 g, 0.6 mmol) in a mixture of MeOH (14 ml) and H₂O (1 ml), K₂CO₃ (0.43 g, 3.1 mmol) was added and the resulting mixture was refluxing for 2 h. The solvent was removed in vacuo, the resulting residue was taken up with H₂O (10 ml) and extracted with CHCl₃ (2 \times 30 ml). The organic solvent was dried and evaporated to furnish a residue that was purified by flash chromatography eluting with a mixture of CH₂Cl₂/MeOH/33% aq. NH₄OH (9/1/0.1) to give **24** as yellow oil: 70% yield; ¹H NMR (CDCl₃, 200 MHz) δ 1.26–1.50 (m, 20H + 2H exch with D₂O), 2.17 (s, 3H), 2.31 (t, J = 7.8 Hz, 2H), 2.69–2.31 (t, J = 7.2 Hz, 2H), 3.46 (s, 2H), 7.29–7.32 (m, 5H).

4.1.22. *N*-Benzyl-12-isothiocyanato-*N*-methylododecan-1-amine (**8**)

To a solution of **24** (0.12 g, 0.39 mmol) in dry CH₂Cl₂ (10 ml), under nitrogen, 1,1'-thiocarbonyldi-2(1H)-pyridone (0.091 g, 0.39 mmol) in dry CH₂Cl₂ (5 ml) was added dropwise and the resulting mixture was stirred at room temperature overnight. The solvent was removed in vacuo and the residue was purified by gravity column eluting with petroleum ether/CH₂Cl₂/MeOH (6/3.5/0.5) to give **8** as yellow oil: 59% yield; ¹H NMR (CDCl₃, 400 MHz) δ 1.26–1.32 (m, 14H), 1.34–1.41 (m, 2H), 1.48–1.52 (m, 2H), 1.62–1.69 (m, 2H), 2.17 (s, 3H), 2.33–2.36 (m, 2H), 3.41–3.48 (m, 4H), 7.21–7.24 (m, 1H), 7.26–7.30 (m, 4H); ¹³C NMR (CDCl₃, 100 MHz) δ 26.36, 27.18, 28.61, 29.20, 29.30, 29.38, 29.41, 29.49, 29.53, 29.80, 41.99, 44.86, 57.36, 62.09, 126.67, 127.95, 128.86, 129.55, 138.91. MS (ESI⁺) m/z = 347 (M + 1H)⁺.

4.2. Biochemistry

4.2.1. Materials and instrumentations

All chemicals were of analytical grade and purchased from Fluka-Sigma-Aldrich S.r.l. (Milan, Italy) with the exception of Amplex Red reagent (10-acetyl-3,7-dihydroxyphenoxazine), purchased from Molecular Probes/Invitrogen (Invitrogen S.r.l., San Giuliano Milanese (MI, Italy)). Recombinant human SSAO/VAP-1 (r-VAP-1) was a kind gift from BioTie Therapeutics (Turku, Finland); it was stored at 4 °C at 0.1 mg/ml, in 10 mM sodium phosphate (pH 7.4) containing Triton X-100 (0.1% v/v).

Human recombinant MAO A and MAO B expressed in baculovirus infected BT1 cells (5 mg/ml) and horseradish peroxidase were purchased from Fluka-Sigma-Aldrich S.r.l. (Italy).

Human adipocyte lysates were prepared from isolated fat cells according to a previously reported procedure [34]. Briefly, after collagenase digestion, cells were lysated using a buffer containing Hepes (20 mM), EDTA (1 mM), Triton X-100 (0.5%) and anti-proteases

(protease inhibitor cocktail, dilution 1/400, v/v) at pH 7.2. The lysates were centrifuged at $15,000 \times g$ for 20 min and the supernatant was stored in liquid nitrogen until use, pellet was discarded. The relative amounts of MAO A and MAO B activity present in lysates were evaluated by measuring amine oxidase activity, after 20 min of pre-incubation with clorgyline (2 μ M) or deprenil (2 μ M), irreversible selective MAO A and MAO B inhibitors, respectively. A control sample, pre-incubated in the absence of inhibitor, was taken as reference. Using tyramine (1 mM) as substrate, the following relative amount of MAO A and MAO B activity were found: 71% of MAO A and 29% MAO B activity, in good agreement with previous studies [52].

The protein concentration of the samples was determined according to the method of Bradford (1976), using bovine serum albumin as standard protein [53].

The stock solutions of the various compounds were prepared in water, with the exception of compound **7**, dissolved in chloroform/methanol (1/1, v/v), and **8** and **5** dissolved in dimethylsulfoxide.

A Cary–Eclipse fluorimeter (Varian Inc., PaloAlto, CA, USA) and a Cary 50 Scan UV–visible spectrophotometer (Varian Inc.) were employed for fluorescence and spectrophotometric measurements, respectively.

4.2.2. Amine oxidase activity assay

Amine oxidase activity was determined by measuring hydrogen peroxide generation rate by a peroxidase-coupled continuous assay. The Amplex Red reagent was used as fluorogenic substrate for horseradish peroxidase [54]. All experiments were carried out in the following “Hepes buffer”: Hepes 50 mM, KCl 50 mM, CaCl_2 2 mM, MgCl_2 1.4 mM, NaCl 120 mM, pH 7.4 [55]. Phosphate buffer was not used to avoid possible formation of phosphate-spermine derivative complexes [56].

Assays were carried out in a final volume of 800 μ l, in the presence of Amplex Red (100 μ M) and horseradish peroxidase type II (5 U ml^{-1}). The solutions containing VAP-1 or MAOs (in the presence or absence of the various compounds), were pre-incubated for 30 min, unless otherwise specified; then the substrate was added and the reaction was run, continuously, for 3 min. As substrates were used benzylamine, for VAP-1 and MAO B, and p-tyramine, for MAO A.

Initial velocities were determined by measuring the increase in fluorescence intensity ($\lambda_{\text{exc}} = 563$ nm and $\lambda_{\text{em}} = 586$ nm); H_2O_2 generation rate was calculated from the change in fluorescence intensity, by means of calibration curves obtained by serial dilution of stock solution of H_2O_2 . In particular, since tyramine decreases the fluorescence intensity generated by the system peroxidase–Amplex red–hydrogen peroxide, the reaction rates of MAO A, at various tyramine concentrations, were calculated using specific calibration curves built for each concentration of the substrate used for the enzyme activity assay.

For each measurement, the corresponding blank, measured in the absence of the substrate, was subtracted. No significant interference of the various compounds on fluorescence intensity was observed.

The pre-incubation and the kinetic assays were performed in air equilibrated solutions, at 30 °C for MAOs and at 37 °C for VAP-1, unless otherwise specified. Under these conditions, the control samples of amine oxidases maintain their enzyme activity, tested under “saturation” condition of substrate.

4.2.3. Kinetic analysis

Steady state kinetic parameters (V_{max} and K_m) were calculated by fitting an appropriate kinetic equation to the experimental data (initial rate of reactions vs substrate concentrations), with Sigma Plot software, version 9.0 (Jandel Scientific, San Rafael, CA, USA) or GraphPad 5.0 software. The Michaelis–Menten equation was

applied to determine the apparent V_{max} and K_m values of MAO A and MAO B in the presence of the various compounds.

As regards VAP-1, in the presence of substrate inhibition, kinetic data were analysed according to Eq. (1) in Holt et al. [15], a simplified form of that reported by Holt et al. [55].

The mode of inhibition was determined by global fit analysis (GraphPad 5.0 software) of the initial rate of reaction versus substrate concentration plots, in the presence and absence of inhibitor, to fit equations for competitive, mixed, non-competitive and uncompetitive inhibition models; the fit giving the highest r^2 value was selected for the calculation of inhibition constants.

All experiments were performed at least in triplicate.

All the reported kinetic parameters and the standard errors of the mean value (S.E.M) are the results of the best-fit of data to the appropriate kinetic equation.

4.2.4. Time-dependent inhibition studies

Recombinant MAO A and MAO B (0.02–0.05 mg/ml) or human adipocytes lysates (0.4 mg/ml) in the Hepes buffer, were pre-incubated for periods from 0 to about 50 min, at 30 °C in the presence and in the absence of inhibitor (control sample). After various time intervals of pre-incubation (at least 5 times after mixing of enzyme and inhibitor), the residual MAOs enzyme activity of samples was determined: an aliquot of sample was withdrawn and diluted in the assay buffer (50-fold dilution) and, after 1 min, substrate was added under “saturating” condition (tyramine 1 mM and BZA 10 mM for MAO A and B, respectively).

All time-dependent inhibition experiments were monitored relative to a control sample, which was run exactly as the experiment except without inhibitor added (only an equivalent volume of solvent used for the tested inhibitor, was added).

The enzyme activity of this control sample (v_0) was set to 100% at each time point and for each time point the ratio between residual enzyme activities (v_{+i}) relative to the control sample (v_0), was calculated. The “apparent inactivation rate constant” values (k'_{obs}), for each inhibitor concentration, were calculated by linear regression analysis of the data of logarithm of residual activity ($\ln(v_{+i}/v_0)$) versus time.

The Kitz and Wilson model [57], shown in Scheme 5, was found to fit the time-dependent inhibition data (k'_{obs} vs inhibitor concentration):



Scheme 5.

In this scheme, a rapid reversible interaction between free enzyme (E) and inhibitor (I) is followed by a slower, irreversible reaction, which transforms the reversible enzyme–inhibitor complex (EI) into an irreversible enzyme inhibitor complex (EI^*). The inactivation rate constant (k_{inact}) and the enzyme–inhibitor dissociation constant (K_{EI}), were calculated by fitting Eq. (1) to the data of “apparent inactivation rate constants” (k'_{obs}) versus $[I]_0$.

$$k'_{\text{obs}} = k_{\text{inact}}[I]_0 / (K_{EI} + [I]_0) \quad (1)$$

4.3. Molecular modelling

Human MAO-A and MAO-B were retrieved from the protein data bank (PDB: 2Z5X and 4A79, respectively). Hydrogen atoms were added to the protein structure using standard geometries with MOE (MOE 2010.10, Molecular Operating Environment, Chemical Computing Group) [58]; to minimize contacts between hydrogens, the structures were subjected to Amber99 force field minimization

until the root mean square deviation of conjugate gradient was $<0.1 \text{ kcal mol}^{-1} \text{ \AA}^{-1}$ ($1 \text{ kcal} = 4.184 \text{ kJ}$; $1 \text{ \AA} = 0.1 \text{ nm}$), keeping the heavy atoms fixed at their crystallographic positions. **8** was built using MOE builder and minimized using PM3 semi-empirical quantum mechanics force field implemented in Mopac 7. A set of docking runs were performed using the program Schrödinger Glide [59]. Molecular dynamics (MD) simulations of the minimized complexes (parameterized with AMBER99) were performed with NAMD 2.8 [60] in order to verify their stability over time; in particular a 30 ns of NPT (1 atm, 300 K) MD simulation were performed after an equilibration phase of 1 ns (positional restraints were applied on carbon atoms to equilibrate the solvent around the protein).

4.4. Biological evaluation

4.4.1. Cell cultures and treatment

Human dopaminergic neuroblastoma *SH-SY5Y* cells were propagated in DMEM supplemented with 10% heat-inactivated bovine serum, 1% penicillin/streptomycin solution and 1% L-glutamine solution (all obtained from Sigma, St. Louis, MO, USA). Cells were treated with different concentrations of **7** or **8** within the following range: 0–500 μM .

4.4.2. Flow cytometry

All flow cytometric analyses were performed by using the easyCyte 5HT flow cytometer (Millipore Guava Technologies, Hayward, CA, USA).

4.4.3. Cytotoxicity test

Cytotoxicity test was performed after 24 h of treatment with different concentrations of **7** or **8**. Briefly, aliquots of 2×10^4 cells were stained with 100 μL of Guava Nexin Reagent (Millipore Guava Technologies, Hayward, CA, USA), containing Annexin V-phycoerythrin (Annexin V-PE) and 7-amino-actinomycin D (7-AAD). After a 20 min of incubation at room temperature in the dark, the samples were analysed by flow cytometry. The inhibitory concentration causing 50% of cell toxicity following one cell-cycle exposure (24 h) (*i.e.* IC_{50}) was estimated by plotting x-y, fitting the data with a linear regression model, and using a curve-fitting software to interpolate the concentration causing 50% of cell toxicity (GraphPad InStat version 5.0, GraphPad Prism, San Diego, CA, USA).

Fundings

This research was supported by institutional grants from the University of Padova-Italy (Fondi di ricerca di Ateneo Ex 60%, codes 60A06-4744/10 and 60A06-9480/11 to M.L.D.P.) and from Italian MIUR, Rome-Italy (PRIN 2009ESXPT2_001).

Acknowledgements

We thank and are very grateful to Prof. Dale E. Edmondson and his coworker, Dr. Milagros Aldeco (Department of Biochemistry, Emory University School of Medicine, Atlanta, U.S.A.), and to Prof. Claudia Binda (Dept. Biology and Biotechnology, University of Pavia, Pavia, Italy) for some experiments and for their useful comments and suggestions.

The authors would like to thank Dr. D.J. Smith and Biotie Therapies Corp. (Turku, Finland) for the kind gift of purified human VAP-1.

We are very grateful to Prof. Stefano Moro (Department of Pharmaceutical Science, University of Padova, Padova, Italy) for kind support.

Appendix A. Supplementary data

Supplementary data related to this article can be found at <http://dx.doi.org/10.1016/j.ejmech.2013.07.005>.

References

- [1] M.B.H. Youdim, Y.S. Bakhle, Monoamine oxidase: isoforms and inhibitors in Parkinson's disease and depressive illness, *Br. J. Pharmacol.* 147 (2006) S287–S296.
- [2] M.B. Youdim, D. Edmondson, K.F. Tipton, The therapeutic potential of monoamine oxidase inhibitors, *Nat. Rev. Neurosci.* 7 (2006) 295–309.
- [3] A. Hald, J. Lotharius, Oxidative stress and inflammation in Parkinson's disease: is there a causal link? *Exp. Neurol.* 193 (2005) 279–290.
- [4] M. Bortolato, K. Chen, J.C. Shih, Monoamine oxidase inactivation: from pathophysiology to therapeutics, *Adv. Drug Deliv. Rev.* 60 (2008) 1527–1533.
- [5] A. Bolasco, S. Carradori, R. Fioravanti, Focusing on new monoamine oxidase inhibitors, *Expert Opin. Ther. Pat.* 20 (2010) 909–939.
- [6] M.S. Song, D. Matveychuk, E.M. Mackenzie, M. Duchcherer, D.D. Mousseau, G.B. Baker, An update on amine oxidase inhibitors: multifaceted drugs, *Prog. Neuropsychopharmacol. Biol. Psychiatry* 44 (2013) 118–124.
- [7] S. Mandel, O. Weinreb, T. Amit, M.B.H. Youdim, Mechanism of neuroprotective action of the anti-Parkinson drug rasagiline and its derivatives, *Brain Res. Rev.* 48 (2005) 379–387.
- [8] O. Weinreb, T. Amit, O. Bar-Am, M. Yogev-Falach, M.B.H. Youdim, The neuroprotective mechanism of action of the multimodal drug lisdostigil, *Front. Biosci.* 13 (2008) 5131–5137.
- [9] S. Carradori, D. Secci, A. Bolasco, P. Chimenti, M. D'Ascenzio, Patent-related survey on new monoamine oxidase inhibitors and their therapeutic potential, *Expert Opin. Ther. Pat.* 22 (2012) 759–801.
- [10] V. Flamand, H.J. Zhao, D.M. Peehl, Targeting monoamine oxidase A in advanced prostate cancer, *J. Cancer Res. Clin. Oncol.* 136 (2010) 1761–1771.
- [11] F. Chimenti, R. Fioravanti, A. Bolasco, P. Chimenti, D. Secci, F. Rossi, M. Yanez, F. Orallo, F. Ortuso, S. Alcaro, R. Cirilli, R. Ferretti, M.L. Sanna, A new series of flavones, thioflavones, and flavanones as selective monoamine oxidase-B inhibitors, *Bioorg. Med. Chem.* 18 (2010) 1273–1279.
- [12] A. Gaspar, T. Silva, M. Yanez, D. Vina, F. Orallo, F. Ortuso, E. Uriarte, S. Alcaro, F. Borges, Chromone, a privileged scaffold for the development of monoamine oxidase inhibitors, *J. Med. Chem.* 54 (2011) 5165–5173.
- [13] M.J. Matos, S. Vilar, R.M. Gonzalez-Franco, E. Uriarte, L. Santana, C. Friedman, N.P. Tatonetti, D. Vina, J.A. Fontenla, Novel (coumarin-3-yl)carbamates as selective MAO-B inhibitors: synthesis, in vitro and in vivo assays, theoretical evaluation of ADME properties and docking study, *Eur. J. Med. Chem.* 63 (2013) 151–161.
- [14] N. Desideri, R. Fioravanti, L. Proietti Monaco, M. Biava, M. Yanez, F. Ortuso, S. Alcaro, 1,5-Diphenylpenta-2,4-dien-1-ones as potent and selective monoamine oxidase-B inhibitors, *Eur. J. Med. Chem.* 59 (2013) 91–100.
- [15] E. Bonaiuto, A. Minarini, V. Tumiatti, A. Milelli, M. Lunelli, M. Pegoraro, V. Rizzoli, M.L. Di Paolo, Synthetic polyamines as potential amine oxidase inhibitors: a preliminary study, *Amino Acids* 42 (2012) 913–928.
- [16] M. Zini, C.L. Passariello, D. Gottardi, S. Cetrullo, F. Flamigni, C. Pignatti, A. Minarini, V. Tumiatti, A. Milelli, C. Melchiorre, C. Stefanelli, Cytotoxicity of methoctramine and methoctramine-related polyamines, *Chem. Biol. Interact.* 181 (2009) 409–416.
- [17] V. Tumiatti, A. Milelli, A. Minarini, M. Rosini, M.L. Bolognesi, M. Micco, V. Andrisano, M. Bartolini, F. Mancini, M. Recanatini, A. Cavalli, C. Melchiorre, Structure–activity relationships of acetylcholinesterase noncovalent inhibitors based on a polyamine backbone. 4. Further investigation on the inner spacer, *J. Med. Chem.* 51 (2008) 7308–7312.
- [18] T. Boncher, X. Bi, S. Varghese, R.A. Casero Jr., P.M. Woster, Polyamine-based analogues as biochemical probes and potential therapeutics, *Biochem. Soc. Trans.* 35 (2007) 356–363.
- [19] A. Minarini, A. Milelli, V. Tumiatti, M. Rosini, M.L. Bolognesi, C. Melchiorre, Synthetic polyamines: an overview of their multiple biological activities, *Amino Acids* 38 (2010) 383–392.
- [20] C. Melchiorre, M.L. Bolognesi, A. Minarini, M. Rosini, V. Tumiatti, Polyamines in drug discovery: from the universal template approach to the multitarget-directed ligand design strategy, *J. Med. Chem.* 53 (2010) 5906–5914.
- [21] S. Jalkanen, M. Salmi, VAP-1 and CD73, endothelial cell surface enzymes in leukocyte extravasation, *Arterioscler. Thromb. Vasc. Biol.* 28 (2008) 18–26.
- [22] M. Unzeta, M. Sole, M. Boada, M. Hernandez, Semicarbazide-sensitive amine oxidase (SSAO) and its possible contribution to vascular damage in Alzheimer's disease, *J. Neural Transm.* 114 (2007) 857–862.
- [23] I. Ferrer, J.M. Lizcano, M. Hernandez, M. Unzeta, Overexpression of semicarbazide sensitive amine oxidase in the cerebral blood vessels in patients with Alzheimer's disease and cerebral autosomal dominant arteriopathy with subcortical infarcts and leukoencephalopathy, *Neurosci. Lett.* 321 (2002) 21–24.
- [24] Y. Zhang, Allyl isothiocyanate as a cancer chemopreventive phytochemical, *Mol. Nutr. Food Res.* 54 (2010) 127–135.
- [25] C. Fimognari, M. Lenzi, P. Hrelia, Chemoprevention of cancer by isothiocyanates and anthocyanins: mechanisms of action and structure–activity relationship, *Curr. Med. Chem.* 15 (2008) 440–447.

- [26] S.J. Jackson, K.W. Singletary, Sulforaphane: a naturally occurring mammary carcinoma mitotic inhibitor, which disrupts tubulin polymerization, *Carcinogenesis* 25 (2004) 219–227.
- [27] Y.S. Keum, W.S. Jeong, A.N. Kong, Chemoprevention by isothiocyanates and their underlying molecular signaling mechanisms, *Mutat. Res.* 555 (2004) 191–202.
- [28] Y.C. Hsu, S.J. Chang, M.Y. Wang, Y.L. Chen, T.Y. Huang, Growth inhibition and apoptosis of neuroblastoma cells through ROS-independent MEK/ERK activation by sulforaphane, *Cell Biochem. Biophys.* (2013), <http://dx.doi.org/10.1007/s12013-013-9522-y>.
- [29] P. Wellendorph, J.W. Jaroszewski, S.H. Hansen, H. Franzyk, A sequential high-yielding large-scale solution-method for synthesis of philanthotoxin analogues, *Eur. J. Med. Chem.* 38 (2003) 117–122.
- [30] G.V. Bobkov, S.N. Mikhailov, A. Van Aerschot, P. Herdewijn, Phosphoramidite building blocks for efficient incorporation of 2'-O-aminoethoxy(and propoxy) methyl nucleosides into oligonucleotides, *Tetrahedron* 64 (2008) 6238–6251.
- [31] M.A. Cinelli, B. Cordero, T.S. Dexheimer, Y. Pommier, M. Cushman, Synthesis and biological evaluation of 14-(aminoalkyl-aminomethyl)aromathecins as topoisomerase I inhibitors: investigating the hypothesis of shared structure-activity relationships, *Bioorg. Med. Chem.* 17 (2009) 7145–7155.
- [32] H. Marom, K. Miller, Y. Bechor-Bar, G. Tsarfaty, R. Satchi-Fainaro, M. Gozin, Toward development of targeted nonsteroidal antiandrogen-1,4,7,10-tetraazacyclododecane-1,4,7,10-tetraacetic acid-gadolinium complex for prostate cancer diagnostics, *J. Med. Chem.* 53 (2010) 6316–6325.
- [33] A. Minarini, A. Milelli, V. Tumiatti, L. Ferruzzi, M.R. Marton, E. Turrini, P. Hrelia, C. Fimognari, Design, synthesis and biological evaluation of new naphthalene diimides bearing isothiocyanate functionality, *Eur. J. Med. Chem.* 48 (2012) 124–131.
- [34] E. Bonaiuto, M. Lunelli, M. Scarpa, R. Vettor, G. Milan, M.L. Di Paolo, A structure-activity study to identify novel and efficient substrates of the human semicarbazide-sensitive amine oxidase/VAP-1 enzyme, *Biochimie* 92 (2010) 858–868.
- [35] D.E. Edmondson, C. Binda, J. Wang, A.K. Upadhyay, A. Mattevi, Molecular and mechanistic properties of the membrane-bound mitochondrial monoamine oxidases, *Biochemistry* 48 (2009) 4220–4230.
- [36] E.M. Milczek, C. Binda, S. Rovida, A. Mattevi, D.E. Edmondson, The 'gating' residues Ile199 and Tyr326 in human monoamine oxidase B function in substrate and inhibitor recognition, *FEBS J.* 278 (2011) 4860–4869.
- [37] C. Carpené, D. Daviaud, J. Boucher, S. Bour, V. Visentin, S. Gres, C. Duffaut, E. Fontana, X. Testar, J.S. Saulnier-Blache, P. Valet, Short- and long-term insulin-like effects of monoamine oxidases and semicarbazide-sensitive amine oxidase substrates in cultured adipocytes, *Metabolism* 55 (2006) 1397–1405.
- [38] A. Zorzano, M. Palacín, L. Marti, S. García-Vicente, Arylalkylamine vanadium salts as new anti-diabetic compounds, *J. Inorg. Biochem.* 103 (2009) 559–566.
- [39] J. Mercader, Z. Iffiu-Soltesz, X. Brenachot, A. Foldi, P. Dunkel, B. Balogh, C. Attane, P. Valet, P. Matyus, C. Carpené, SSAO substrates exhibiting insulin-like effects in adipocytes as a promising treatment option for metabolic disorders, *Future Med. Chem.* 2 (2010) 1735–1749.
- [40] F. Hubalek, C. Binda, A. Khalil, M. Li, A. Mattevi, N. Castagnoli, D.E. Edmondson, Demonstration of isoleucine 199 as a structural determinant for the selective inhibition of human monoamine oxidase B by specific reversible inhibitors, *J. Biol. Chem.* 280 (2005) 15761–15766.
- [41] A.P. Vintem, N.T. Price, R.B. Silverman, R.R. Ramsay, Mutation of surface cysteine 374 to alanine in monoamine oxidase A alters substrate turnover and inactivation by cyclopropylamines, *Bioorg. Med. Chem.* 13 (2005) 3487–3495.
- [42] E.M. Milczek, D. Bonivento, C. Binda, A. Mattevi, I.A. McDonald, D.E. Edmondson, Structural and mechanistic studies of mofegiline inhibition of recombinant human monoamine oxidase B, *J. Med. Chem.* 51 (2008) 8019–8026.
- [43] R. Borštnar, M. Repič, M. Kržan, J. Mavri, R. Vianello, Irreversible inhibition of monoamine oxidase B by the antiparkinsonian medicines rasagiline and selegiline: a computational study, *Eur. J. Org. Chem.* 32 (2011) 6419–6433.
- [44] R.M. Geha, K. Chen, J. Wouters, F. Ooms, J.C. Shih, Analysis of conserved active site residues in monoamine oxidase A and B and their three-dimensional molecular modeling, *J. Biol. Chem.* 277 (2002) 17209–17216.
- [45] B. Kacar, D.E. Edmondson, Studies on the role of lysine-296 in human mitochondrial monoamine oxidase B catalysis, *FASEB J.* 20 (2006) A478–A479.
- [46] C. Binda, A. Coda, R. Angelini, R. Federico, P. Ascenzi, A. Mattevi, A 30-angstrom-long U-shaped catalytic tunnel in the crystal structure of polyamine oxidase, *Structure* 7 (1999) 265–276.
- [47] G. Zhao, R.C. Bruckner, M.S. Jorns, Identification of the oxygen activation site in monomeric sarcosine oxidase: role of Lys265 in catalysis, *Biochemistry* 47 (2008) 9124–9135.
- [48] G. Zhao, Oxygen activation in flavoprotein oxidases: the importance of being positive, *Biochemistry* 51 (2012) 2662–2669.
- [49] S.Y. Son, A. Ma, Y. Kondou, M. Yoshimura, E. Yamashita, T. Tsukihara, Structure of human monoamine oxidase A at 2.2-angstrom resolution: the control of opening the entry for substrates/inhibitors, *Proc. Natl. Acad. Sci. U. S. A.* 105 (2008) 5739–5744.
- [50] R. Saiki, Y. Yoshizawa, A. Minarini, A. Milelli, C. Marchetti, V. Tumiatti, T. Toida, K. Kashiwagi, K. Igarashi, In vitro and in vivo evaluation of polymethylene tetraamine derivatives as NMDA receptor channel blockers, *Bioorg. Med. Chem. Lett.* 23 (2013) 3901–3904.
- [51] E. Agostinelli, M. Condello, A. Molinari, G. Tempera, N. Viceconte, G. Arancia, Cytotoxicity of spermine oxidation products to multidrug resistant melanoma M14 ADR2 cells: sensitisation by the MDL 72527 liposomotropic compounds, *Int. J. Oncol.* 35 (2009) 485–498.
- [52] N. Pizzinat, L. Marti, A. Remaury, F. Leger, D. Langin, M. Lafontan, C. Carpené, A. Parini, High expression of monoamine oxidases in human white adipose tissue: evidence for their involvement in noradrenaline clearance, *Biochem. Pharmacol.* 58 (1999) 1735–1742.
- [53] M.M. Bradford, A rapid and sensitive method for the quantitation of microgram quantities of protein utilizing the principle of protein-dye binding, *Anal. Biochem.* 72 (1976) 248–254.
- [54] M. Zhou, N. Panchuk-Voloshina, A one-step fluorometric method for the continuous measurement of monoamine oxidase activity, *Anal. Biochem.* 253 (1997) 169–174.
- [55] A. Holt, D.J. Smith, L. Cendron, G. Zanotti, A. Rigo, M.L. Di Paolo, Multiple binding sites for substrates and modulators of semicarbazide-sensitive amine oxidases: kinetic consequences, *Mol. Pharmacol.* 73 (2008) 525–538.
- [56] A. Corazza, R. Stevanato, M.L. Di Paolo, M. Scarpa, B. Mondovi, A. Rigo, Effect of phosphate ion on the activity of bovine plasma amine oxidase, *Biochem. Biophys. Res. Commun.* 189 (1992) 722–727.
- [57] R. Kitz, I.B. Wilson, Esters of methanesulfonic acid as irreversible inhibitors of acetylcholinesterase, *J. Biol. Chem.* 237 (1962) 3245–3249.
- [58] C.C.G. Molecular Operating Environment (MOE2009.10), 1255 University St., Suite 1600, Montreal, Quebec, Canada H3B 3X3.
- [59] Glide, Schrodinger, Inc., New York, NY, 2009.
- [60] J.C. Phillips, R. Braun, W. Wang, J. Gumbart, E. Tajkhorshid, E. Villa, C. Chipot, R.D. Skeel, L. Kale, K. Schulten, Scalable molecular dynamics with NAMD, *J. Comput. Chem.* 26 (2005) 1781–1802.